Project funded by the European Commission under the 6th (EC) RTD Framework Programme (2002- 2006) within the framework of the specific research and technological development programme “Integrating and strengthening the European Research Area”

Project UpWind

Contract No.:
019945 (SES6)

“Integrated Wind Turbine Design”

Author:	Melanie Hau
Affiliation:	Institut für Solare Energieversorgungstechnik (ISET)
Address:	Königstor 59, D-34119 Kassel
Tel.:	+49 561 7294379
Email:	mhau@iset.uni-kassel.de
Further Authors:	
Reviewer:	Martin Geyler
Approver:	

Document Information

Document Type	Deliverable 5.2
Document Name:	Promising Load Estimation Methodologies for Wind Turbine Components
Revision:	
Rev.Date:	
Classification:	
Status:	

Abstract: The first part of this report gives an overview on the loads on important turbine components and the sensor signals, which can be used for load estimation. The second part deals with the field of load estimation and includes promising estimation methodologies for several component load cases.

Contents

STATUS, CONFIDENTIALITY AND ACCESSIBILITY											
Status				**Confidentiality**				**Accessibility**			
S0	Approved/Released			**R0**	General public			Private web site			
S1	Reviewed			**R1**	Restricted to project members			Public web site			
S2	Pending for review			**R2**	Restricted to European. Commission			Paper copy			
S3	Draft for commends			**R3**	Restricted to WP members + PL						
S4	Under preparation			**R4**	Restricted to Task members +WPL+PL						

PL: *Project leader* **WPL:** *Work package leader* **TL:** *Task leader*

1. Introduction

In the past 20 years, the wind turbines available on the market increased both in diameter and hub height, which allows for higher possible power outputs. However, for strict geometric scaling, the total mass rises disproportionally in comparison to the power, which would lead to an according disproportional rise in material (e.g. steel) consumption. In consequence, more effort is made to realise a lightweight component design, i.e. the components are optimised with respect to material consumption; component strength is only provided where necessary. Aside from this development, turbine and component reliability becomes more important against the background of planned offshore operation.

The continuous estimation of mechanical during turbine operation can help to meet this problem in two ways.
The first refers to the field of condition monitoring: By means of a continuous recording of the estimated loads acting on a turbine component, both the monitoring of occurring extreme load amplitudes and of fatigue loads is possible. Fatigue load assessment can be carried out by means of a fatigue cycle counting process, e.g. applying the rainflow method. The combination of estimated load amplitudes and numbers of cycles can be compared to the component's Wöhler curve. It is thus possible to estimate a component's residual life time, which could be taken into account for both the maintenance strategy and the turbine operational control. Besides, the recorded fatigue and extreme loads can provide a feedback to turbine design, allowing to verify the load spectrum used for component dimensioning. If the load monitoring is meant only for an long-term influence on the operation, off-line data processing is sufficient. In contrast, if a rapid influence on the operational control is intended, data processing has to be done on-line, i.e. during operation with little time lag.
Second, load estimation gives the opportunity to influence the loads directly: The estimated information about acting loads can be used for load reducing control algorithms. E.g. the generator torque/ pitch controllers could additionally target at load reduction, using the estimated loads as input signals. However, this second objective requires a real-time estimation.
Generally, component load estimation is an alternative to measurement action, which can also provide the mentioned advantages. However, detailed measurements are often intricate and costly. Estimations could also form a redundant system for load evaluations when used in parallel with measurements.

A wind turbine is a complex mechanical-electrical system, which both interacts with its environment and features various interaction processes between its components. See Figure 1 for a schematic description. The present wind field is the most important input parameter, it largely determines the turbine's operation. Second, the influence of the connected electrical grid is very important, since it dictates the needed feed-in frequency and voltage. Additional environmental influences are unavoidable disturbances, such as wave impact or gravity.
Aiming to turn the wind's momentum into a torque on the generator, the wind field first causes aerodynamic forces on the rotor, which influence the structural motion of the turbine. Apart from the intended torsional movement of the generator, oscillations are excited involving many structural components of the turbine. The generator torque magnitude, which is set by the generator control, also influences the turbine component's structural motion. Structural motion in turn influences the aerodynamic forces on the blades. This effect is called aeroelastic coupling. This is also true for the present pitch angles, which are determined by the pitch controller according to current operation conditions.
The mentioned interactions and the volatile wind field make it difficult to estimate the operational loads of a wind turbine. Depending on the component and the load case, a load estimation algorithm relies on one or several measured signals.

The first part of this report gives an introduction to the loads on important turbine components and the sensor signals, which can be used for load estimation. The second part deals with the

field of load estimation and includes promising estimation methodologies for several component load cases.

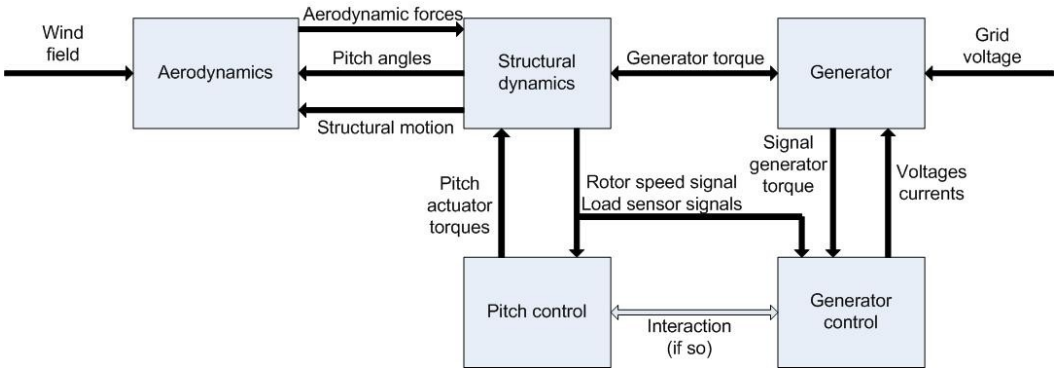

Figure 1: *Schematic of Interactions during Wind Turbine Operation*

2. Overview Over the Main Loads Occurring in Wind Turbines

When regarding the behaviour of a mechanically loaded component, one has to distinguish between two load quantities: external loads and internal loads.
The term *external load* refers to forces on the component which are determined by the component's surroundings. These are first environmental loads acting directly on the component, e.g. aerodynamic forces and gravity on a rotor blade. Second, the term includes loads which are caused by interactions with other turbine components, either passively provoked by the turbine structure or actively induced by the turbine control, e.g. pitch actuator torques.
In connection with a component's structure and dynamic behaviour, external loads lead to local loads in the component, i.e. stress and deformations, see schematic in Figure 1. These are here called *internal loads*; an example is the bending stress at the blade root. For one-dimensional components, such as slender beams, local internal loads can be described by three quantities: normal forces, shear forces and bending moment.

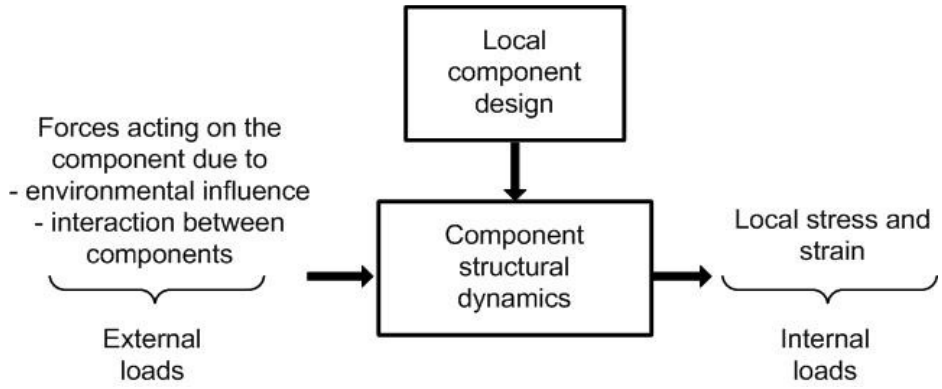

Figure 2: *Relation Between External and Internal Loads on a Turbine Component*

The internal loads are decisive for the component life. Generally speaking, if the internal loads exceed the material's maximum load limit, failure will result. This load limit is characteristic for each material. Two different types of internal load limits have to be considered and the arising internal load cases are commonly categorized according to the affected type of load limit.
The first type is characterised by extremely high load magnitudes which can cause a component failure the first time they act on it. The loads are thus called *extreme loads*. Several parameters exist to describe the material's capability to accept extreme load magnitudes. E.g. the yield stress of a material gives the maximum stress value which can be applied without leading to a plastical deformation of the material. However, since material parameters are based on certain stress directions, some effort is necessary to compare internal load magnitudes with material parameters. Complex, polyaxial internal loads have to be converted into so-called *comparison stresses*, which give equivalent uniaxial stress values.
On the other hand, loads with a relatively low amplitude in comparison to the extreme load amplitude can cause a fatigue fracture in materials when applied over a large number of load cycles. That means, the occurring load cycles accumulate during the component's life; the combination of load amplitude and load cycle number specifies this so-called *fatigue load*. For many materials, a relation between the internal load amplitude and the number of load cycles which lead to a fatigue fracture is given by the Wöhler curve.
One of these two load types will be the design load, i.e. the load which determines the component's material and dimensions during design process.

The basis of component design are the external loads that must be expected to arise during the turbine's life (typically 20 years). Each turbine component has to be designed such that it can withstand both singular extreme loads (e.g. the maximum external load magnitude occurring during 10 seconds in 50 years) and fatigue loads, thus load oscillations.
The expected internal loads can be calculated for a chosen component design. The extreme loads can be translated into a tensile stress value which in turn can be compared to the material's maximum load magnitude. Dynamic simulations may be necessary, too, e.g. to determine the turbine response to a certain type of wind gust. Determining the internal fatigue loads requires more effort: a dynamic load analysis is carried out and the results are processed applying a so-called fatigue cycle counting method, e.g. the rainflow method: The arising loads are arranged in several classes, according to their amplitudes and the number of cycles is counted for each class. The result can be compared with the material's Wöhler curve.
In an iteration loop, the turbine component must be designed such that the material's maximum acceptable extreme and fatigue loads are higher than the resulting internal loads at each point of the component.
However, it is difficult to estimate the occurring amplitudes and numbers of both external and internal load cycles for a turbine's design life, since they strongly depend on the wind characteristics at the site. This fact and additional insecurities in material behaviour and calculations is allowed for by taking a safety factor into account.
It is obvious that a component's design again influences the whole turbine's dynamic structure and thus external loads which act on other components. Thus, further iteration loops are necessary in turbine design.

Component oscillations, which are a main cause of fatigue loads, can generally be divided into two types, *forced oscillations* and *natural oscillations*:
An external load acting on a component causes a component response, i.e. deformation. Oscillating external loads thus make a component oscillate with the external load's frequency (forced oscillations). As will be shown in the following sections, such oscillating external loads play an important role in wind turbine component design. In particular, due to the finite number of blades, many component external loads pulsate with the blade passing frequency, which equals the triple rotor frequency for three bladed turbines (3p). Regarding the blades themselves, load variations at the 1p frequency is very significant.
If a component's mode is excited, the component will also oscillate, but with the according eigen frequency and mode shape (natural oscillation). If no further excitation happens, the oscillation decays according to the respective damping ratio. Components can e.g. be excited by load steps, which contain all frequencies and thus excite all modes of a component. The resulting component motion is in fact a superposition of its mode shapes at the according eigen frequencies, decaying with the according damping ratios.

2.1 Loads on the Rotor Blades

The purpose of the rotor is to turn a share of the wind's momentum into a torque on the turbine main shaft. This leads to aerodynamic forces acting on a blade, which can be divided into a drag and a lift component for each blade element, resulting in the aerodynamic thrust and the torque acting on the hub. The causing quantity is the relative wind speed vector, which results from the absolute wind speed vector and the structural motion of the blade element in question. Its angle with respect to the blade chord determines the coefficients of lift and drag, which in turn influence the amplitude of the according forces.
Aerodynamic forces present a main cause of external loads to the blade. They contain a strongly fluctuating load component, originating from several effects:

- The wind field, which consists of the wind speed vectors existing at the rotor area, varies over time. This leads to fluctuating aerodynamic forces and loads on a blade, no matter if in motion or at standstill.
- During rotation, the blade periodically experiences the existing wind speed vectors at each point in the rotor area. Since the wind field is not homogeneous, i.e. the absolute

values and directions at a time are not the same for each point in the rotor area, the aerodynamic forces on the blade vary due to the blade's rotation. Thus, even a time-constant wind field causes load fluctuations, which are periodical with rotor frequency. In particular, wind shear, yaw misalignment and the tower shadow effect cause such periodic fluctuations.

- Since the aerodynamic forces depend directly on the rotor speed, a variation of rotor speed also causes a fluctuation of the aerodynamic forces. This point is only significant for variable wind speed turbines, where the rotor speed can be influenced by means of control.
- In pitch regulated wind turbines, variations of aerodynamic forces are induced intentionally by changing the pitch angle and with it the angle of attack.

Besides the aerodynamic forces, two other relevant environmental loads act on the blades, which are caused by gravity and centrifugal forces.
Gravity acts constantly on the blades with direction to the ground, but it leads to a different resulting external load for each blade position. As long as the blade rotates, the load is fluctuating periodically with the rotor rotational frequency.
The centrifugal forces appear only during rotor turning. The load acts radially, directed away from the centre of rotation and varies with the rotor speed.
Important interaction loads arise during pitch actuator action and because of changes of the generator torque.

For each blade element, a strong and a weak principal axis can be determined in the profile plane. They are characterised by the maximum and the minimum geometric moment of inertia respectively. These axis are orthogonal to each other and they indicate the so-called flapwise and edgewise directions. At the three-dimensional blade, they set the directions of flexural vibrations: blade bending occurs about the weak and the strong principal axis in each element, which is called the flapwise and edgewise bending respectively. However, the axis directions change over the blade span, which is mainly due to the blade's twist. This is why edgewise and flapwise bending and deflections can not be assigned to a fix direction with respect to e.g. the blade root. The mode shapes are thus more complex than e.g. for an axially symmetric beam, since they are three-dimensional instead of being limited to a plane.
An alternative system of directions, which is fix for a blade, is based on the rotor plane. The according directions are the so-called in-plane direction and the out-of-plane direction. The first is a tangential vector to the blade element's path, while the latter is a vector perpendicular to the rotor plane. As Figure 2 shows, this system of directions differs from the flapwise-edgewise system by the angle θ, which varies with the blade radius and the pitch angle.

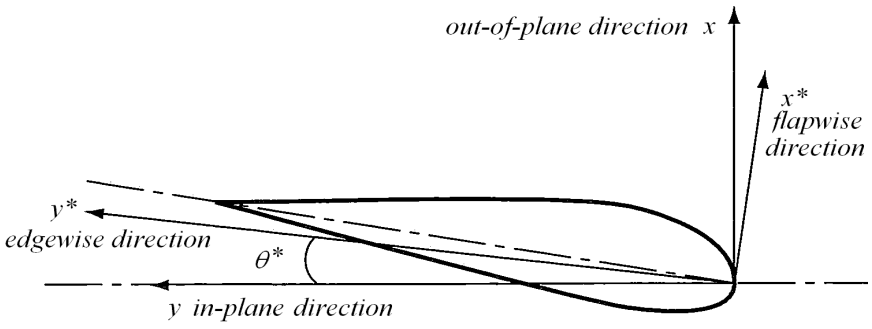

Figure 3: *Edgewise and Flapwise Direction at a Rotor Blade Element*

Four main types of internal load result from the external loads mentioned above: flapwise bending, edgewise bending, radial forces and torsion.

Blade flapwise bending has various causes, which are

- Aerodynamic forces in flapwise direction:
  The largest component of these forces is formed by the aerodynamic thrust force. The resulting internal load contains both a constant and a fluctuating component. The first occurs already at constant external load, i.e. a homogeneous and constant wind field without a tower shadow effect etc. The fluctuating internal load component is due to fluctuation of aerodynamic forces, i.e. varying relative inflow velocity.
- Flapwise natural oscillations:
  Fluctuating internal loads occur after flapwise mode excitation by either of the mentioned forces.

Due to the small difference between the flapwise direction and the out-of-plane direction, small components of the following forces also cause a small component of flapwise bending loads:

- Gravitational forces
  A small component of gravitational forces causes flapwise bending. Due to rotation, this external load generally fluctuates and so does the resulting internal load.
- Changes in rotor speed, induced by the generator torque control:
  In connection with the blade inertia, rotor deceleration or acceleration also leads to forces on the blade in in-plane direction. A small component of these induces flapwise bending, resulting in an internal bending load.

The material stresses due to flapwise bending loads are especially high due to the blade geometry, featuring relatively small blade dimensions to support flapwise bending (moment of inertia). The loads e.g. originating from thrust at extreme wind conditions can form an extreme internal load. The fluctuating bending at moderate amplitudes presents a fatigue-type internal load. Both load types are important for the blade design.

Similarly, edgewise bending originates from different external loads, namely

- Gravitational forces:
  They cause the largest component of edgewise bending. Particularly for small pitch angles, gravitational forces have a large edgewise component. Because of the blade rotation, the resulting internal bending load oscillates at rotor frequency.
- Aerodynamic forces in edgewise direction:
  The constant component of these forces creates a constant internal bending load. For a varying relative inflow velocity, the resulting internal loads feature a fluctuating component. However, large component of edgewise forces act tangentially to the blade's orbit, creating the aerodynamic torque. Since the blade mounting is not fixed but rotates, the resulting internal loads are significantly lower than the actual aerodynamic forces would suggest.
- Changes in rotor speed, induced by the generator torque control:
  A large component of tangential forces arising due to a change of rotor speed acts in edgewise direction and thus induces edgewise bending.
- Edgewise natural oscillations:
  After excitation of an edgewise mode, natural oscillations will result, causing internal bending loads.

The combination of relatively high magnitudes and the large number of load cycles due to gravitational forces cause the edgewise bending to be a fatigue type load.

When it comes to bending, a rotor blade in principle behaves like a bending beam which is clamped at one end. If all edgewise and all flapwise acting forces have the same sign respectively throughout the rotor span, the resulting bending moments will add up towards the clamped end and become maximal at the blade root. This is generally the case for wind turbine

operation[1], thus the flapwise and edgewise bending moments at the blade root can serve as an indication for the internal bending load of the whole blade. However, it can not reflect the bending stresses at the individual points over the blade span.
The edgewise/flapwise blade root bending moments are often transferred to the in-plane/out-of-plane system of directions. This offers the advantage, that these bending moments can more easily be related to some operating parameters and resulting loads for other components. E.g. the blade out-of-plane bending moment leads to the aerodynamic thrust, which forms a part of the tower external load. The blade in-plane bending moment in turn is related to the aerodynamic torque and gravitational forces.
However, as mentioned above, the current angle between weak axis and rotor plane has to be taken into account for converting the bending moments or forces to the other system of directions.

Radial forces on the blade are caused by centrifugal forces and by gravity. The first is a constant radial force if the rotor speed is constant. Both rotor speed variation and in particular gravity cause a fluctuation of radial forces during operation. Evidently, the highest resulting radial internal loads exist at the blade root.

The torsional external load acting on the blade root is characterised by the existing torsional moment. Again, there are various causes:

- Pitch action:
  The pitch actuator imposes a torque on the blade in order to change the pitch angle. The highest torque occurs at the blade root. The internal load fluctuates as well as the external one.
- Aerodynamic forces:
  If the present aerodynamic forces at a blade element don't have their resulting point of application in the pitch axis, they create a moment about the pitch axis, which in turn leads to an internal torsional load.
- Deflection from the rotor plane:
  If the blade is deflected from the rotor plane and thus from the original pitch axis, the gravitational and tangential aerodynamic forces (which act parallel to the rotor plane and perpendicular to the pitch axis) create a moment about the original pitch axis. This moment depends on the distribution of the mentioned forces and the deflection over the span.
- Torsional natural oscillations
  If an excitation of a torsional mode is caused by an external load, the blade oscillates about its pitch axis according to the excited torsional mode.

Because of the last three aspects, the torsional load does not necessarily reach its maximum at the blade root for local torsional moments can partly compensate each other with respect to the blade root.

Figure 4 contains a schematic of a wind turbine and the most important mentioned loads on a rotor blade.

2.2 Loads on the Rotor Hub

Being the joint between blades and main shaft, the rotor hub experiences external interaction loads from the blades and from the drive train. Since it is fix with respect to the hub, the rotor-plane-based system of directions is suitable to describe the occurring loads.
The hub has to stand both the out-of-plane and the in-plane blade bending moments at the blade root as well as the torsional and radial forces on the blade. These present external loads to the hub, which attack at the blade mountings, generally featuring the same fluctuations.

1 strictly speaking, e.g. second mode natural oscillations show a different characteristic

These external hub loads can therefore be determined if the the blade root loads are known, see Section 2.1.
Besides, the drive train can induce interaction loads, caused by drive train torque fluctuations e.g. due to control action.

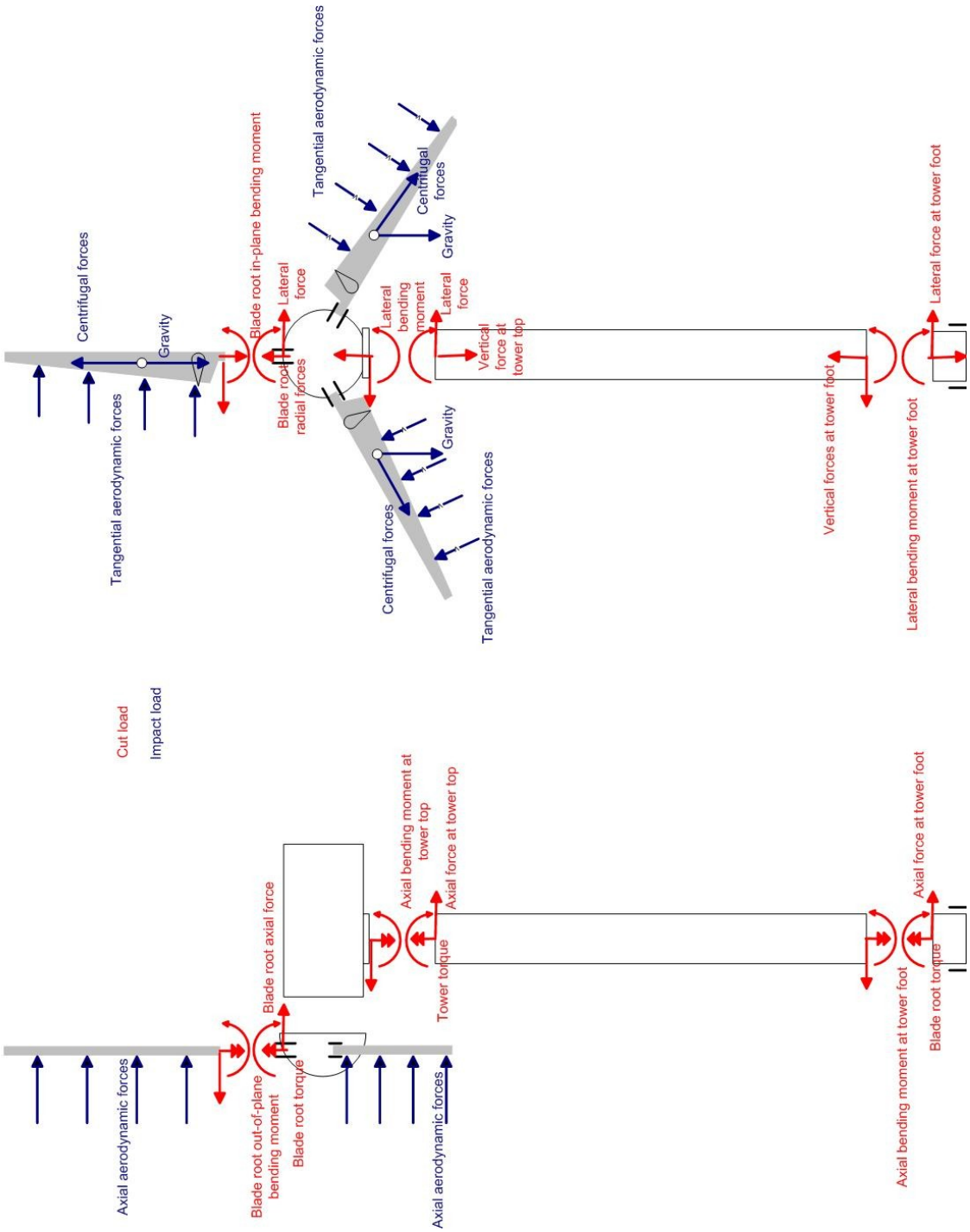

Figure 4: *Important External Forces and Moments Acting at a Wind Turbine; Internal Forces, Moments and Torques at Highly Loaded Spots*

2.3 Loads on the Main Shaft and Main Bearings

The main shaft of a wind turbine links the rotor hub to the gearbox or, for turbines without gearbox, to the generator. In wind turbines with gearbox, it is called low-speed shaft due to its lower speed in comparison to the fast-speed shaft between gearbox and generator. Two bearings support the main shaft, while it transmits the angular momentum to the drive train. The main shaft thus is exposed to external interaction loads induced by the hub and by the drive train.
During operation, for fluctuating wind speed, a dynamic torsional load acts on the shaft: A rise in wind speed increases the rotor aerodynamic torque. This increase is transmitted to the main shaft, which is thus affected by a torsional load. Such dynamic torsional loads, presenting fatigue type loads, are particularly important in fixed-speed wind turbines. In variable-speed turbines, the situation is less critical, since they allow a certain change in rotor speed, which can be used for reducing this dynamic load. By accelerating the rotor, its large moment of inertia is used to short-time-store surplus angular momentum. This way, the torque transmitted to the shaft and drive train is smoothed, as well as the transmitted power.
Torque fluctuations imposed by the generator may also lead to a drive train torsional load.
Further, drive train torsional oscillations can be caused e.g. by aerodynamic torque fluctuations, causing interaction loads on the main shaft.
For constant rotor torque and constant generator torque, the torsional load on the shaft is constant and rather not significant. The internal loads which result from dynamic torsional external loading fluctuate form a fatigue type load.

Main shaft bending during operation occurs due to forces acting on the rotor which are not symmetric with respect to the main shaft axis. Because of rotation, the constant gravitational forces on the rotor lead to a rotating bending moment on the shaft. Apart from that, blade out-of-plane bending moments are transmitted to the shaft via the hub. If all three blades experience the same blade out-of-plane moments, they compensate each other with respect to the shaft. If not, a resulting bending moment acts on the shaft. Due to deterministic effects like wind shear, it fluctuates with a periodic component. It can be split up into a vertical and a lateral component, see Figure 4.

The main bearings support the main shaft with respect to bending and axial forces. They are thus exposed to external interaction loads induced by the main shaft. The first main bearing is located closer to the hub, the second closer to the gearbox, see Figure 4. Alternatively, the second bearing can be integrated into the gearbox. The bearings usually consist of an inner and an outer ring, with rolls between them (roller bearing). The outer ring is attached to the nacelle, the inner ring is attached to the shaft and thus rotates with it. The rolls rotate both around their own axis and the main shaft's axis. Most bearing damages occur due to attrition on the rolls' orbits, i.e. at the inner side of the outer ring and the outer side of the inner ring.
The bearings have to support radial forces which are caused by aerodynamic forces on the rotor and by the rotor mass. One of the bearings additionally supports the axial forces caused by the rotor thrust. The bending moments originating from gravity or a constant tilt moment lead to vertical forces on both bearings, acting contrariwise. They present a constant load to the outer bearing rings, while the inner rings experience a periodically fluctuating load. But since tilt moments are usually not constant, they also lead to a fluctuating load on the outer rings.
Analogous, yaw moments on the rotor lead to lateral forces on the bearings, where for the outer and inner ring the same is true as for the tilt moment.
The rotor thrust leads to axial forces on one of the bearings. The load course corresponds to the thrust force, implying high possible magnitudes.

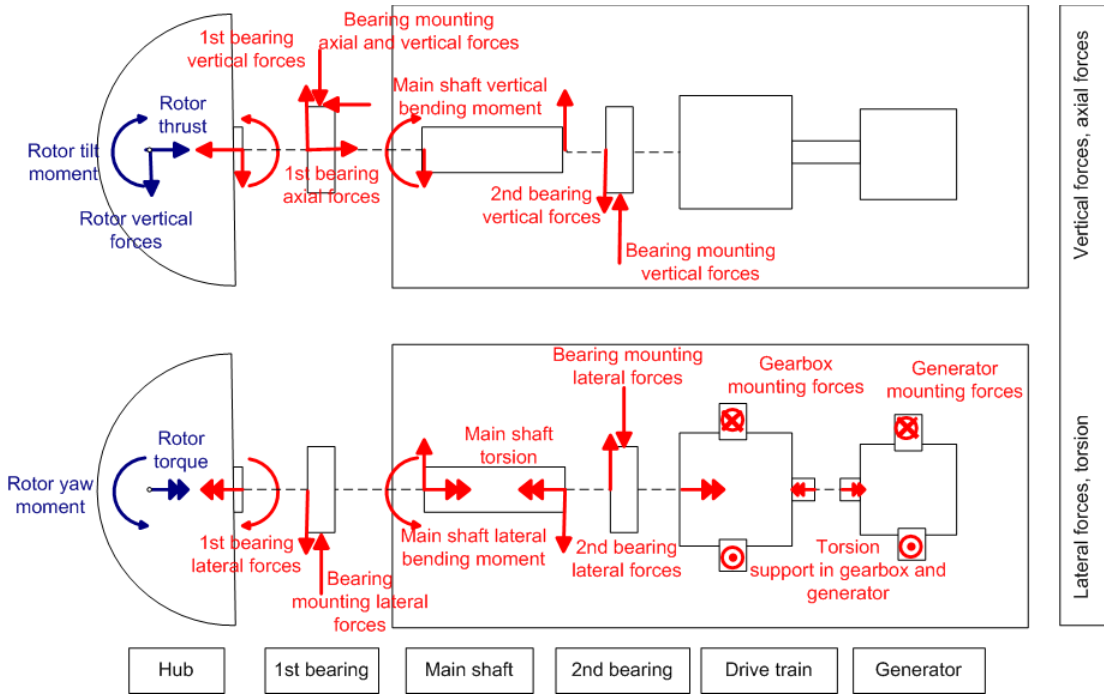

Figure 5: *Forces, Bending Moments and Torques for Nacelle Components; Lateral View (Top) and Top View (Bottom)*

2.4 Loads on the Drive Train

The drive train consists of the gearbox and the fast-speed-shaft, connecting the latter to the generator. Its purpose is to transform the main shaft's speed to the generator speed and to transmit the created torque to the generator. Thus, the decisive external load acting on the drive train is torsional load induced by the main shaft and by the generator. Although the gearbox consists of numerous components, which all experience different external loads, these loads are here not analysed in detail. However, the gearbox torsional load can be considered representative.

Similar to the main shaft, the torsional load is constant during steady-state operation. Fluctuations of the torque to be transmitted lead to a fluctuating component in the torsional load, see also Section 2.3.

2.5 Loads on the Yawing Unit

The yawing unit's purpose is to arrange the turbine orientation which is requested by the turbine control. It is exposed to external loads from the nacelle and from the yaw motor. The yaw drive consists of a horizontally positioned yaw bearing with an internal gear. E.g. the bearing's outer ring is attached to the nacelle, the inner ring to the tower. An electric or hydraulic motor drives a pinion via a gearbox and thus turns the nacelle with respect to the tower. Several brakes ensure a fix yaw position if no yaw movement is requested. During yaw action, in order to smooth the motion, the motor works against intentionally imposed friction, provided e.g. by friction pads.

A yaw moment acting on the rotor must be supported by the yaw brake. Yaw moments on the one hand occur due to yaw errors, but more important are differential loadings on the blades, which cause cyclic yaw moments at a frequency of 3p. [5]/Ch.7

During yaw action, the yaw drive gearbox and the pinion have to transmit the momentum and have to stand the occurring yaw moments, together with the friction imposing device.

Strain measurements can again help to detect the torsional load on the yawing unit.

Furthermore, a tilt moment acting on the rotor, e.g. due to yawed inflow, must be supported by the yawing bearing. Tilt moments vary with the wind field and thus present a fluctuating load.

2.6 Loads on the Tower

The Tower is exposed to external interaction lods which are transmitted by the nacelle. Wind forces also induce some external loading directly on the tower, however, they have a comparatively small effect.

The main external load on the tower is formed by axial bending moments, caused by:

- Out-of-plane aerodynamic forces
  The aerodynamic thrust on the rotor, which depends on the relative inflow velocity and the present pitch angle, is the decisive cause of axial tower bending. Thrust forces acting on the hub, nacelle and the tower itself are much less significant.
  If the out-of-plane aerodynamic forces create a tilt moment on the main shaft, e.g. due to wind shear, this tilt moment acts as an additional external axial bending load on the tower.
  For a constant aerodynamic thrust and tilt moment, the resulting internal loads on the tower are constant. However, wind speed and pitch angle changes lead to load fluctuations. In particular, the tower shadow effect causes fluctuations of out-of-plane aerodynamic forces at blade passing frequency (3p). This leads to forced oscillations of the tower and thus of the internal bending load.
- Gravitational forces
  Gravity acting on the hub and the blades leads to a bending moment, which is constant with respect to the tower. It thus causes a constant axial bending load, but it acts contrariwise to the wind-shear-caused tilt moment.
- Natural oscillations
  Both pitch action and wind speed variations (turbulence) can excite axial tower bending modes via thrust and tilt moment variation. In particular, the first mode is damped only very lightly by structural damping, e.g. with a logarithmic decrement of 0.02 for a welded steel tower. Aerodynamic damping at the rotor increases the total damping significantly; so the total damping reaches a logarithmic decrement of e.g. 0.14. [5]/Ch.5

Due to high possible magnitudes of aerodynamic thrust, the axial tower bending load on the one hand is an extreme type load. However, due to permanent oscillations, fatigue examinations are also important.

Not only axial but also lateral bending leads to significant internal tower loads. This is caused by the torque which must be accepted by the gearbox and generator mountings. A constant torque only causes a small, constant moment attacking in lateral direction at the tower top. Torque fluctuations cause fluctuating lateral moments. In particular, an excitation of the second tower bending mode might occur, leading to natural tower oscillations. Since the rotor does hardly provide aerodynamic damping when it comes to lateral oscillations, the total damping is much smaller than for the axial oscillations. Hence, in spite of lower exciting magnitudes, similar bending magnitudes can be reached as for axial oscillations [5]/Ch.5. Thus, lateral bending presents a fatigue-type load.

Since a wind turbine turns its axis according to the existing wind direction, which usually is not constant, the axial and lateral bending moments act on the tower in varying directions – this again leads to (long term) fluctuations of internal loads.
The relevant forces and moments which cause tower bending all attack at the tower top, hence the highest tower bending moment occurs at the tower foot.

Apart from bending, also torsion presents a load to the wind turbine's tower. It occurs when a torque is induced on the tower by the nacelle, caused by a yaw moment on the rotor. Besides,

yaw action also causes a torque on the tower, however, this is less significant due to small acceleration values.

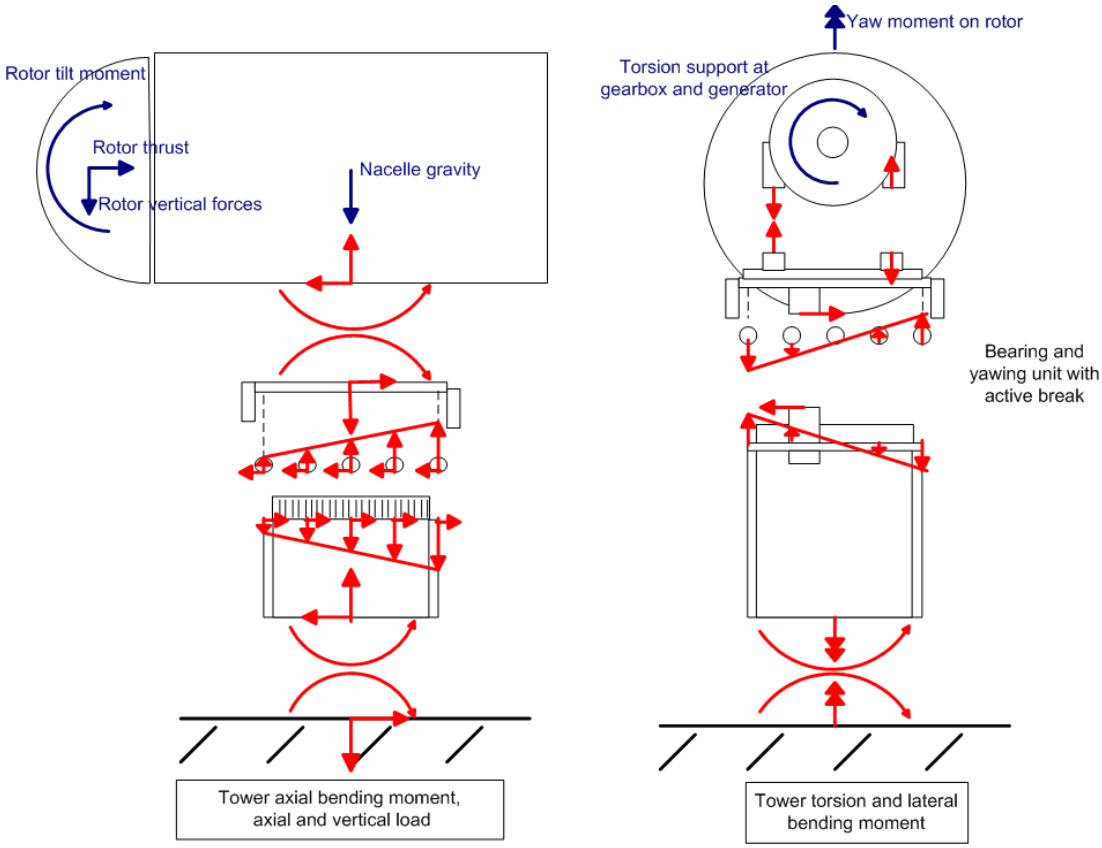

Figure 6: *Forces, Bending Moments and Torques at the Tower Top and Tower Foot*

3. Available Sensor Signals

In order to detect the loads acting on the turbine's main components, suitable measurement signals are necessary. In today's wind turbines, various sensors are installed, quantifying important operating parameters. These measures are utilized in the turbine operating control, the generator and pitch controller or for condition monitoring purposes.
Some of these measurements are expected be useful for load estimation. It is thus important to get an overview on the available sensor signals in today's large wind turbines.

3.1 Rotor Speed and Position

Rotor speed can reliably be measured using inductive proximity sensors. With the help of an inductor, an alternating electromagnetic field is created at the sensor. The sensor is geared to the metal bolts of the flange mounting the hub. Each time a bolt passes the sensor, it influences the oscillating electromagnetic circuit. This is detected by the sensor and a pulse is generated.
The pulse signal frequency gives the rotor speed value n (in rpm) according to:

$$n = \frac{f_{signal}}{N_{bolts}} \cdot 60 \frac{s}{min}$$

The signal is necessary for the turbine control (speed control) and for condition monitoring purposes. The minimum pulse frequency should be at least 5 Hz, N_{bolts} must be chosen accordingly. The speed value should be detected at least 3 times per second (i.e. 3 Hz minimum refreshing rate).
The rotor's absolute position can be measured similarly. As well, an inductive proximity sensor is utilized, but installed so that it only faces one bolt (or an equivalently countable device) per revolution and thus generates only one pulse.

Another way to measure speed and position is to use an incremental encoder, permitting a higher resolution with additional interim values. For this, an incremental disc printed with bright/dark segments is fixed at the device to be observed and rotates with it. A homogeneously segmented track on the disc is used for the rotor speed measurement. Another track only is provided with the zero-position-segment, which serves as basing point for position detection. The encoder photoelectrically scans the tracks and gives both speed and angular position. The data can be retrieved via communication line or analogue output.

Table 1: *Characteristics of Suitable Sensors for Rotor Speed and Position Measurement*

Quantity	***Measurement***	***Signal***	***Accuracy***	***Typical Sampling Time***	***Range***	***Resolu-tion***	***Costs***
Rotor speed	inductive proximity	pulse	1%	100 Hz	0-30 rpm	Depends on N_{bolt}	50€ - 100€
Rotor position	inductive proximity	pulse	5%	100 Hz	0-360°	Depends on N_{bolt}	50€ - 100€
Rotor speed and position	incremental encoder	pulse, data, analogue		100 Hz	0-30 rpm, 0-360°		< 1000€ incl. signal processing unit

3.2 Generator Speed and Position

Both generator speed and position are typically measured with inductive proximity sensors or with incremental encoders, see Section 3.1. The signal is used for condition monitoring purposes and for the generator controller (field oriented control). It must thus feature a high accuracy.

Table 2: *Characteristics of Suitable Sensors for Generator Speed and Position Measurement*

Quantity	***Measurement***	***Signal***	***Accuracy***	***Typical Sampling Time***	***Range***	***Resolution***	***Costs***
Generator speed and position	Incremental encoder	HTL	1024 to 3072 counts per turn	100 Hz	0..3000 rpm, 0..360°	e.g. 0.18° at 2048 counts per turn	850 €
Fast shaft speed for CM	Inductive proximity	pulse	5%, 15% Hysteresis	100 Hz	0..3000 rpm	Depends on $N_{bolt,}$ e.g.12	100€

3.3 Electrical Power

The generator electrical power output signal is necessary for both the turbine control and the generator controller and is apart from that used for condition monitoring purposes. It is calculated as an internal value by the generator control, based on current and voltage probes.

Table 3: *Characteristics of Suitable Methods for Electrical Power Measurement*

Quantity	***Measurement***	***Signal***	***Accuracy***	***Typical Sampling Time***	***Range***	***Resolu-tion***	***Costs***
Electrical Power	Power transducer	analogue	1%	10Hz	$-0.5P_n$ to $+1.5P_n$		1500€
Electrical Power	Inverter	Data (field bus)	<1%	100 Hz	$-0.5P_n$ to $+1.5P_n$		-(inverter internal value)

3.4 Wind Speed

The wind speed is usually measured with the help of an anemometer placed on the top of the nacelle. At this location, the vector is highly disturbed due to rotor turbulence; the signal can thus not be expected to adequately reflect the free wind speed on the rotor surface. The standard is mechanical measurement with cup anemometers. A propeller with three wind-capturing cups rotates around a vertical axis, the number of revolutions per minute allows to calculate the wind speed. It is obvious that this principle contains inaccuracies due to inertia. Since cup anemometers are sensitive to icing, they are often equipped with electrically heated shafts and cups.

For measuring the wind speed components in two or three dimensions, ultrasonic or laser anemometers are recently available. They use the fact that wind speed influences the velocity of sound or light propagation. Since there are no moving parts, maintenance and wear don't present a problem. The measurement principle leads to precise results, not being disturbed by inertia influences. Apart from wind speed, such anemometers also measure the wind direction, see Section 3.5. These facts lead to a rising application of sonic anemometers. However, sensor heating is still necessary if the ambient conditions imply the danger of icing. Another problem is the sensor's sensitivity to mechanical deformation which can be caused e.g. by ice droppings on the sensor.
The wind speed information is used by the turbine control (detection of the cut-in and cut-off wind speed) and for condition monitoring: The accuracy which is necessary for these features is low enough to use cup anemometers.

Table 4: *Characteristics of Suitable Sensors for Wind Speed Measurement*

Quantity	***Measure-ment***	***Signal***	***Accuracy***	***Typical Sampling Time***	***Range***	***Sensiti-vity***	***Costs***
Wind speed	Cup anemometer	Digital/ analogue	+-3% of reading or +-0.5m/s	100 Hz	0.5-50m/s	<0.1m/s	300€
Wind speed	Cup anemometer	Digital/ analogue	+-2% of reading or +-0.3m/s	100 Hz	0.3-60m/s	<0.1m/s	500€
Wind speed and direction	Ultrasonic anemometer	Digital or analogue	+-0.1m/s rms for v<5m/s +-2% of reading (rms) for v>5m/s	100 Hz	0-65m/s (2-dimen-sional)	0.1m/s	1500-2000€

3.5 Wind Direction

The current wind direction is required for the turbine to be positioned optimally with respect to the wind flow. It is an input value to the turbine control, which controls the yawing process. Additionally, the value is interesting for condition monitoring (data classification).
Measurement devices for wind direction detection are usually also located on top of the nacelle, which implies a distortion due to the rotor turbulence. The most common way is to use a wind vane. The vane's position is detected by a potentiometer or an opto-electronic grey code encoder.
For a higher accuracy, the wind direction can be measured in combination with the wind speed, using ultrasonic or laser anemometers, see Section 3.4. While two-dimensional sonic anemometers are able to measure the wind direction within the horizontal plane only, a three-dimensional anemometer gives the spacial wind direction, including a possible vertical component.

Table 5: *Characteristics of Suitable Sensors for Wind Direction Measurement*

Quantity	***Measurement***	***Signal***	***Accuracy***	***Typical Sampling Time***	***Range***	***Sensiti-vity***	***Costs***
Wind direction	Wind vane	Analogue/ digital	+- 5°	100 Hz	0..360°		350€
Wind direction	Wind vane	Analogue/ digital	1.5° , 2.5°	100 Hz	0..360°		850€
Wind speed and direction	Ultrasonic anemometer	Digital or analogue	+-1,0°	100 Hz	0..360°	<=1°	1500-2000€

3.6 Tower Top Acceleration

The tower top acceleration is detected with the help of an acceleration sensor which is placed on the machine bed plate. The signal is an input to the turbine control, used for monitoring tower oscillations.
So-called piezoresistive acceleration sensors apply the piezoresistive effect, stating that the influence of mechanical forces leads to a change in a metal's or a semiconductor's specific resistance. A seismic mass is attached to a beam arrangement with piezoresistors. Acceleration moves the mass and leads to mechanical stress on the sensor's piezoresistors. The change of resistance gives the acting force and thus the acceleration. Both static and dynamic acceleration can be measured (0 Hz to 2 kHz). (3)
Piezoelectric sensors are based on the piezoelectric effect which says that certain materials generate a voltage in response to applied mechanical stress. A seismic mass is mounted directly on a piezoelectric crystal. Acceleration causes a force on the material. With the help of an electronic circuit, the sensor's output signal is made proportional to acceleration. Piezoelectric sensors are applicable for measuring acceleration frequencies down to approximately 0.1 Hz, but not for measuring static acceleration. However, their frequency range is broad. Since they don't contain moving parts, they are very robust. Besides, the measurement principle doesn't require a power supply.
Capacitive acceleration sensors consist of two fixed capacitor plates and a movable capacitor plate (seismic mass) between them. The latter is moved due to occurring acceleration; this change of position leads to a change of capacity. Measurements of 0 Hz signals is possible. However, their measurement principle makes them sensitive to EMC.
Both piezoresistive and capacitive acceleration sensors are also available as so-called MEMS (Micro Electrical Mechanical Systems). I.e., the sensor's mechanical structure (seismic mass, bending beams) is fabricated by micromechanical etching.

Sometimes, tower top oscillations are monitored with the help of the gearbox vibration sensors, see Section 3.7.

Table 6: *Characteristics of Suitable Sensors for Acceleration Measurement*

Measurement	***Signal***	***Accuracy***	***Bandwidth***	***Range***	***Sensitivity***	***Transverse Sensitivity***	***Costs***
Piezo-resistive	Analogue	+-5%	0-250Hz	±2g	8-20mV/g	±2% Span	
Piezo-resistive/ MEMS	Analogue		0-100 Hz (±5%)	±3g	700mV/g	<3%	850€ incl. cable
Piezoelectric (quarz) installed at gearbox			0.1 Hz - 10 kHz (+-3dB)	+-500m/s^2 =+-50g	53.5µA/g (+-3%)		300€ incl. cable
capacitive	Analogue		0-20Hz(3dB)	±2g	±1,75pF/g ±40%	5%	30 €
capacitive	Analogue	+-0.05g drift, 2%sensitivity	0-25Hz	±0.5g	200mV/g	3%	
capacitive	Analogue	Nonlinearity <+-1%, thermal sensitivity +- 2%	0-100Hz	+-2g		<3%	

3.7 Gearbox Vibration

The gearbox vibration is measured for condition monitoring purposes. In order to monitor the gearbox vibrations three-dimensionally, several sensors can be installed at the gearbox, aligned in different spacial directions. Vibration can be understood as high-frequency acceleration, for which piezoelectric acceleration sensors are ideal. They can e.g. cover mechanical vibrations in a frequency range of 3Hz to 20kHz with one sensor only.
Gearbox vibration sensors can also help to detect tower top oscillations, if their sensitivity to low frequency acceleration is high enough. Noted lateral or axial vibrations at a tower eigen-frequency at least serve as an indication.

Table 7: *Characteristics of Suitable Sensors for Gearbox Vibration Measurement*

Measure-ment	***Signal***	***Accuracy***	***Bandwidth***	***Range***	***Sensitivity***	***Transverse Sensitivity***	***Costs***
Piezoelectric acceleration sensor	analogue	5%	3 Hz - 20kHz	+/-20g	100mV/g		
Piezoelectric vibration sensor (PCB)	analogue		0.2 Hz - 10kHz (+-3dB)	±50g	100mV/g	≤ 5%	450€ incl. cable

Measure-ment	***Signal***	***Accuracy***	***Bandwidth***	***Range***	***Sensiti-vity***	***Transverse Sensitivity***	***Costs***
Piezoelectric / ceramic shear	analogue		0.53 Hz - 15 kHz	±50g	100mV/g	≤ 5%	
Piezoelectric /shear			10%: 0.7Hz-25kHz	±100g(I)	50mV/g± 2%(I)	≤ 5%(I)	
Piezoelectric (quarz)			0.1 Hz..10 kHz (+-3dB)	±50g	53.5µA/g		300€ incl. cable

4. Possible Future Sensor Signals

As stated in Section 1, emerging loads on wind turbines rise with turbine sizes and reliability becomes more and more important. This is why turbine manufacturers and operators might tend to install more sensors in future wind turbines, in order to improve condition monitoring systems and to help the turbine control to operate the turbine more gently. However, it is important to note that sensor installation is not only costly due to investment and maintenance, but sensor faults themselves might lead to a turbine malfunction.
Measurements which might be carried out in future wind turbines include the following.

4.1 Blade Root Strains

The strain due to bending at the blade root is an interesting signal when it comes to load reducing interventions in wind turbine operation. The blade root bending is an indicator for mechanical load acting on the whole blade, which typically acts in two directions, flapwise and edgewise. The according strain signals could be used for monitoring the static and oscillation blade load, as an input for the turbine control and also for pitch controlling.
The standard strain measurement method is to use strain gauge resistor bridges as sensors in combination with signal amplifiers. Strain gauges are resistors, which change their resistance when strain occurs to them. This is first due to the resulting change of geometry and second due to the piezoresistive effect (see also Section 3.6). Strain gauges are attached to the object to be observed and experience the same strain as the object at the particular point.
Since strain gauges are sensitive to ageing and corrosion, their long term stability is unsatisfactory and thus they are not suitable for the use through the 20 years of a wind turbine's design life. Apart from this, due to the necessity to use long electrical cables and amplifiers with high gain factors, EMC can be a problem.
An alternative to common strain gauges are fibre optic strain gauges such as Fibre Bragg Grating sensors. Its basis is a fibre containing a so called bragg grating. That is, the fibre's structure and with it its reactive index was changed permanently in periodic distances.
This grating causes a particular fibre behaviour in terms of reflection and transmission: Light of the wavelength λ_B (the “bragg wavelength”) will be partly reflected at each grate period, leading to a constructive superposition. The resulting spectrum of reflection has its peak at the bragg wavelength, while the spectrum of transmission shows a gap in the same range. λ_B depends on the grate's period length, which in turn is influenced by mechanical strain (deformation) acting on the fibre among others.
By sending broad-band light through sensor fibre, its reflection characteristics are noticed. After detecting λ_B from the spectrum of reflection, the strain can be calculated.(4)
Since this technology is relatively new on the market, it is just starting to be used in the field of wind energy. Tests promise a good behaviour regarding long-term stability, fatigue durability and electrical immunity (5), which makes them a valuable tool for condition monitoring and control purposes.
However, the blade in-plane bending could be detected in another way: knowing the aerodynamic torque and the position of each blade, it is possible to calculate the blade root bending moment at each blade. The aerodynamic torque can be detected by measuring the main shaft torque.
As for the radial loads acting at the blade root, it could equivalently be measured with the help of strain gauges. Another way here is to calculate the load from the measured rotor speed signal and a position signal for each blade.

Table 8: *Characteristics of Applicable Sensors for Strain Measurement*

Measurement	***Signal***	***Noise***	***Measurement frequency***	***Range***	***Resolution***	***Costs***
Resistive Strain gauges						5000-6000€
Fibre Bragg Grating Sensor	data/ analogue	1.7με	500Hz	±4500με	0.8 με	15 000€
Fibre Bragg Grating Sensor	data/ analogue		25 Hz for 20 sensors	+-4000με	0.8με	30 000€ - 40 000€

4.2 Tower Foot Strains

Analogue to the blade root strain, the tower foot strain due to bending is an indicator for the mechanical load acting on the tower structure. Again, there are typically two directions, the axial direction (parallel to the turbine's main shaft) and the lateral direction, which is perpendicular to the main shaft. Both static and oscillation loads must be expected. The signal can be used for condition monitoring, as input to the turbine control and to the pitch controller.
Regarding the availability and suitability of sensors, the same things apply which are mentioned in Section 4.1.

4.3 Blade Tips Acceleration

Out-of-plane oscillation is an important load to a wind turbine's blades and it also has an impact on the turbine itself. In order to monitor this blade oscillation, acceleration sensors could be implemented at the blade tips. The available acceleration sensors are mentioned in Section 3.6.
A problem which arises when trying to detect out-of-plane blade acceleration is the existing centripetal acceleration due to rotation, $a_r = r \cdot \omega^2$. Since acceleration sensors always show also a certain sensitivity to acceleration in directions other than the direction to be measured (e.g. 3%) , and radial acceleration usually reaches high values in comparison to flapwise acceleration, measurement errors would occur. An additional problem occurs due to blade bending: A sensor could be mounted such that its measurement axis is perpendicular to the blade axis. Thus, the sensor's measurement axis is only perpendicular to the rotor plane (out-of-plane direction), if the blade axis lies within the rotor plane. For any blade deflection from the rotor plane, e.g. due to bending, the measurement axis is not pointing to the desired out-of-plane direction, but deviates from it by an angle φ. This again would introduce a measurement error. See Table 6 for characteristics of selected acceleration sensors.

4.4 Yaw and Tilt Moment

The yaw and the tilt moment acting on the rotor leads to bending of the main shaft and causes strain at the gearbox mounts. Hence, detecting the occurring strain at these mounts is a possibility to indirectly measure these values. Another way of indirect measurements is to use individual blade root strain measurements and the position of each blade if these data are available.
Strain can be detected using conventional strain gauge resistor bridges or optical strain sensors, see Section 4.1 and Table 8.

4.5 Shaft torque

Highly dynamic wind gusts cause important mechanical loads at the main shaft and the drive train components. The shaft torque is related to the generator torque which can easily be detected from the generator current signal. But this signal does not contain the mentioned dynamic fluctuations, since they are smoothed out. So in order to monitor these loads, the torque could be measured at the main shaft or at the fast speed shaft.
If a torque is transported through a shaft, it causes a small twisting at the shaft. This twisting can be measured with the help of strain sensors, see Section 4.1, allowing to calculate the torque. For this measurement, four sensors are applied to the shaft shell in the direction of the principal stresses. In detail, two pairs of strain gauges are applied oppositely, each containing two sensors. In each pair, one of the sensors is aligned + 45° and the other - 45° from the shaft axis projection to the shaft shell. A twisting causes compression at one and stretching at the other strain gauge element in each pair, which can be detected. The signals are transferred telemetrically with the help of transmitter mounted on the rotating shaft. An inductive power supply can be used to provide the necessary power to the installation on the rotating shaft.
The measurement equipment causes both high costs and installation effort. Since the data transfer equipment is sensitive to EMC and other environmental influences, and conventional strain gauges show a lack of long term stability, calibration and maintenance lead to additional costs.
Since resistive strain gauges are sensitive to ageing and corrosion, fibre-optical strain gauges could be a suitable alternative. See Table 8 for information on the sensors.

5. Load Estimation Approaches Reported in Literature

A literature study was carried out on the state of the art in load estimation. Both the field of wind turbines and other industries were regarded.

5.1 Load Estimation in the Field of Wind Turbines

Wind speed, being one of the most important input parameters to the system “wind turbine”, plays an important role for the loads on the turbine structure and thus for load estimation. Since it behaves eratically and is not distributed homogeneously over the rotor surface, its magnitude is difficult to obtain. The common way of wind speed detection by means of an anemometer only takes into account one location of the rotor area and the values are significantly falsified by the rotor itself. More detailed and reliable information about the undisturbed wind field would provide significant advantages e.g. in the field of load-reducing control.
This is why approaches to estimate wind speed are here reported as well as those to estimate mechanical loads on wind turbines.

In [10], wind speed is proposed to be estimated using the measured signals of rotor speed, generator speed and generator electrical power: In a first step, the rotor aerodynamic torque and power are estimated from generator speed and electrical power, taking into account the drive train characteristics. The wind speed can then be estimated by solving the non-linear relation

$$\hat{P}_R = \frac{\rho}{2} \cdot A_R \cdot c_p\left(\frac{\omega_R \cdot R}{\hat{v}}, \beta\right) \cdot \hat{v}^3$$

where c_p is a function of the estimated tip speed ratio λ and the pitch angle β, being characteristic for the blade profile. The equation can e. g. be solved by iteration and yields a unique solution for non-stall conditions.
This method yields one magnitude for the “effective wind speed”, a substitutional value for the whole wind field, which is assumed to be homogeneous and directed perpendicular to the rotor area. The estimated wind speed value was proposed to be included in the generator torque control.
Besides, the estimated rotor aerodynamic power and the estimated wind speed both serve as a basis for reconstructing the rotor aerodynamic thrust force. The current pitch angle and the blade characteristics (power coefficient and thrust coefficient) are necessary input signals:

$$\hat{F}_T = \frac{c_s(\hat{\lambda}, \beta)}{c_p(\hat{\lambda}, \beta)} \frac{\hat{P}_R}{\hat{v}}$$

Similarly, the blade aerodynamic flapwise moments are reconstructed according to

$$\hat{M}_f = R \frac{c_{M_{ax}}(\hat{\lambda}, \beta)}{c_p(\hat{\lambda}, \beta)} \frac{\hat{P}_R}{\hat{v}}$$

where the c_{Max} is the blade coefficient of flapwise moment. However, the estimated value neglects asymmetric wind fields. The tower foot bending moment and the flapwise blade root bending moment can be calculated if the turbine structural mechanics are neglected.
Furthermore, utilising the estimated rotor aerodynamic torque, the main shaft torsional moment is approximated according to:

$$\hat{M}_{ts} = \hat{M}_R \frac{J_G}{J_{tot}} + M_G \frac{J_R}{J_{tot}}$$

A very similar approach for wind speed estimation is reported in [16]. Two possibilities are described to solve the nonlinear relation, here between wind speed and reconstructed rotor aerodynamic torque: first by means of on-line iteration as in [10] and second by implementing a three-dimensional lookup-table. The latter implies the necessity for interpolation between the lookup-table values. Here, the estimated wind speed is fed into the pitch control in order to improve power regulation above rated.

In [4], observers are mentioned as a methodology to estimate a particular variable during wind turbine operation, based on a model of the according dynamics. E.g. the wind speed acting on the rotor may be estimated from the measured power and/or the rotational speed and the pitch angle.
Furthermore, state estimators are proposed for estimation of several system states. They incorporate a Kalman Filter with a complete model of the turbine dynamics; the estimation process is based on the difference between measured system parameters and their estimated correspondent. Stochastic (Gaussian) elements in the real system can be taken into account, which suggests to include a Gaussian wind speed model.

Several authors use this state-space estimation methodology for wind speed estimation.
E.g. in [14], wind speed disturbance is estimated for a DTC torque controller, tracking the optimum tip speed ratio, only considering wind fields which are normal to and uniform over the rotor disk. In [17], state estimation is largely applied in disturbance accommodating control. E.g., an appropriate model is shown to estimate the uniform wind speed and rotor speed from measured generator speed. Control performance is improved by taking into account more related states and measurements. Wind speed is generally modelled as step disturbance, either uniform over the rotor disc or individually for each blade.

In [1], which deals with modelling and controlling a wind turbine with the help of fuzzy-linked, locally valid linear controllers, the author uses linear, locally valid Kalman estimators to acquire the states of the nonlinear wind turbine system. In order to achieve a better controller performance, he estimates wind speed by including it into his state estimators as a disturbance. At this, he proposes to model wind speed as a sampling system.

There are several reports in the field of blade monitoring. [7] reports a monitoring system for the rotor blade, which allows to detect cracks and gives information about the blade's fatigue life status. This is facilitated with the help of fibre bragg grating strain sensors, which detect the strain acting at selected points of the blade. Additionally provided with information on the pitch angles, rotor speed and rotor position, the monitoring system calculates the blade load situation and the average wind speed in front of the rotor. By means of a rainflow counting process, the blade's fatigue life status is continuously estimated.
Besides, several FBG sensors are installed at blade regions which are sensitive to cracks. Cracks will lead to sensor failure, which makes both crack appearance and continuation detectable.
All information is provided to the turbine control system and the turbine operator.

Also, [12] reports research on blade monitoring systems which are based on fibre bragg grating strain sensors. Strain and blade root bending moments are measured, a rainflow counting process allows the assessment of the blade fatigue lifetime. The retrieved load spectra are proposed to be compared with other turbines on the site or with the design case. Costs and reliability are considered as a obstacle of FBG sensor systems to be widely applied.

In [18], a method for damage detection is proposed which utilizes the proportionality of maximum dynamic strain and maximum oscillation velocity of a given mechanical structure with

respect to a specific mode shape. Since the factor of proportionality is characteristic for a system but will react sensitively in case of a damage, synchronous strain- and velocity measurements allow for damage diagnosis, e.g. at a turbine tower.

5.2 Load Estimation in Other Fields than Wind Energy

In [9] the authors use a disturbance estimator for their method to reduce engine-induced vibrations in automotive vehicles by active control. The vibrations which are induced to the vehicle by the engine (disturbance) are aimed to be compensated by an actuator. The residual vehicle vibrations (error) are measured by means of an accelerometer. The estimator is designed as a stationary Kalman filter; an input disturbance model is included which describes the engine-induced vibrations. The disturbance frequencies are harmonics of a basic frequency which in turn depends on the current engine frequency. This is why the disturbance model and the observer gain need to be adapted to the current engine operating point; both are chosen according to an engine-frequency schedule.

In [2] a method is proposed to estimate mechanical loads acting on an aircraft during the flight. Besides, velocities of disturbances to the steady-state flow conditions such as gusts or turbulences are reconstructed. The basis is a modified Kalman filter, which contains a nonlinear model of the aircraft, including an input disturbance model. In addition to standard measurement signals in commercial aircrafts (e.g. the plane's Euler angles), the measurement vector contains the vertical and lateral velocities and accelerations of the plane's centre of gravity.

[8] reports a methodology to estimate empennage in-flight-loads of a small aircraft with the help of backpropagation neural networks. The aim was to predict tail loads with as few sensors as possible, especially avoiding the need of strain gauges on the airplanes. In order to acquire training and testing data for the neural networks, a plane was equipped with strain gauges and potential input data sensors (such as linear and angular accelerometers). Data were collected during several types of maneuvers and various airspeeds. Two neural networks were trained and tested: one for the horizontal tail and one for the vertical tail. Four acceleration signals (angular acceleration with respect to all three axes plus z-axis linear acceleration) were considered sufficient to achieve a good load estimation performance for the regarded air plane type.

In [11] the authors propose a so-called smartsensor for a mechanical system, which is able to estimate vibrational loads on the system with the help of response signals from sensing elements (accelerometers). The sensor is based on a neural network; its performance was tested for load estimation in the front landing gear of a small transport air plane during landing. Before, the neural network was trained with load data (obtained by means of strain gauges on the wheel suspension) and according structure response data (accelerometer signals placed on the landing gear fixture).

According to [15], air loads on helicopter blade sections were estimated with the help of measured data on the leading edge pressure and several operational parameters (such as the tip Mach number and the shaft angle of attack). Two methodologies were tested as load estimation algorithms: linear regression and a neural network model. The influence of several parameters and pressure measurement locations on estimation performance was analysed.

Another way to determine loads and structural response of an aircraft is proposed in [13]. Given surface strain data are fed into an inverse interpolation process which is based on a finite element model of the given airframe. Starting from a parametric approximation of the loading, a least-squares-minimization process is carried out for the calculated and the given strain data.

6. Promising Methods for Load Estimation in Wind Turbine Components

As reported in Section 5, there are three in principle different approaches in literature when it comes to load estimation during operation.
Several approaches can be pooled as “inverse model methodologies”. They reconstruct load data from measured system response data by means of a physical model which is applied inversely.
A second methodology is the use of state-estimators/ Kalman filters, which requires a dynamic model of the (sub)system in question. Estimation is continuously corrected by using the estimation error (difference between estimated and measured system outputs) as estimator input. This methodology allows to estimate both system states and input disturbances.
The third method incorporates a neural network, which needs to be trained first e.g. with experimental data, namely load signals (to-be output signals) and according response signals of the system (to-be input signals). The neural network does require physical knowledge about the system in the form of a system model.

In order to make use of the available physical knowledge on the wind turbine, the suggested estimation approaches will be based on physical models of the wind turbine's subsystem in question.

Generally speaking, wind turbines are vibratory systems. Many of the main turbine components themselves tend to perform significant oscillations during operation. Such oscillations lead to a significant internal load component and have thus to be considered when component loads are estimated. For example, the axial tower foot bending moment in a certain direction is caused by the external thrust force and dynamically influenced by the tower inertia:

$$M_{b,\,towerft}(t) = F_{th}(t)\cdot H - \int_0^H m(h)\cdot \ddot{x}(h,t)\cdot h\,dh \qquad (1)$$

The static thrust force component leads to a static load component, while its dynamic fluctuation and the inert force component result in a dynamic load component. Load cases with an important component of inertial forces include tower bending, blade bending and drive train torsional load.
However, in some load cases, component oscillations don't contribute significantly to the internal component loads, e.g. if an external load on a component is constant. Even though an external load fluctuates with respect to the component, the component might not perform relevant oscillations if no modes are excited and the component is generally not vibratory with respect to the load case. Examples include the blade radial loads, the main shaft bending load, bearing loads and the tower top axial bending moment caused by rotor gravity.
The estimation methodology has to be chosen according to the load case characteristics: If component oscillations can be neglected, the internal loads can be calculated using a “static” physical model. The loads can be calculated directly either from the known static or dynamic external load or from measured component reactions (“inverse model”).
For load cases with a significant contribution of component oscillation, a state-space estimator is suitable. The suggested general approach is documented in Section 6.1. Then, both information on the causing external force and a signal reflecting the component's motion are necessary.

6.1 General Load Estimation Approach Considering Component Structural Oscillations

6.1.1 Modal Analysis and Modal Condensation

For a simplified treatment, a component's continuum is parted in a suitable number *n* of segments along the main axis. Using the displacement and shear angle at each element boundary as degrees of freedom, the discrete equation of motion is e.g. for a one-dimensional bending beam:

$$\boldsymbol{M}\begin{pmatrix}\ddot{x}_1\\ \ddot{x}_2\\ \vdots\\ \ddot{x}_{(2n+2)}\end{pmatrix}+\boldsymbol{K}\begin{pmatrix}\dot{x}_1\\ \dot{x}_2\\ \vdots\\ \dot{x}_{(2n+2)}\end{pmatrix}+\boldsymbol{S}\begin{pmatrix}x_1\\ x_2\\ \vdots\\ x_{(2n+2)}\end{pmatrix}=\begin{pmatrix}p_1(t)\\ p_2(t)\\ \vdots\\ p_{(2n+2)}(t)\end{pmatrix} \tag{2}$$

where

M	global mass matrix
K	global damping matrix
S	element stiffness matrix
x_i	global degrees of freedom
p_i	global generalized forces

In order to describe the behaviour of a one-dimensional bending beam element, the element's displacement vector is $\boldsymbol{u_j(t)}$ has to contain the relevant degrees of freedom:

$$\boldsymbol{u}_j^T(t)=\{w_0(t),\beta_0(t),w_1(t),\beta_1(t)\}_j \tag{3}$$

with

w	displacement at the respective element boundary
β	shear angle at the respective element boundary

It is connected with the internal loads on element *j* via :

$$[-Q_0(t)\quad -M_{b0}(t)\quad Q_1(t)\quad M_{b1}(t)]_j^T=\boldsymbol{S_j}\cdot\boldsymbol{u_j}(t)+\boldsymbol{M_j}\cdot\ddot{\boldsymbol{u}}_j(t)-\boldsymbol{p_j}(t) \tag{4}$$

where

$\boldsymbol{S_j}$	element stiffness matrix
$\boldsymbol{M_j}$	element mass matrix
Q	local shear force
M_b	local bending moment
$\boldsymbol{p_j}$	vector of generalized force

This relation follows the principle of virtual displacement for a beam element; damping is neglected. For details see [6]. In analogy, in order to dynamically estimate local internal moments and forces, information on the both displacement and shear angle and respective accelerations is required as well as the external force and moment for each element boundary.

If the damping is purely proportional, Equation (2) can be transformed using $\boldsymbol{x}(t)=\boldsymbol{P}\cdot\boldsymbol{r}(t)$:

$$\boldsymbol{M}_{diag}\ddot{\boldsymbol{r}}(t)+\boldsymbol{K}_{diag}\dot{\boldsymbol{r}}(t)+\boldsymbol{S}_{diag}\boldsymbol{r}(t)=\boldsymbol{P}^{T}\boldsymbol{p}(t) \tag{5}$$

where the transformation matrix $\boldsymbol{P}$ contains the mode shape vectors: $\boldsymbol{P}=[\boldsymbol{v}_1\ \boldsymbol{v}_2\ ..\ \boldsymbol{v}_n]$, which contain both degrees of freedom, i.e. deflection and shear angle at each element boundary.
This so-called *modal analysis* leads to *n* independent (decoupled) equations within Equation (5), each describing one mode for one degree of freedom. The modal quantities r_j and $\ddot{r}_j$ can be calculated independently while e.g. the total deflection or the total shear angle x at an element boundary is the weighted sum of the modal quantities:

$$\begin{pmatrix} x_1 \\ x_2 \\ \vdots \\ x_{(2n+2)} \end{pmatrix} = \begin{pmatrix} v_{11} & v_{21} & .. & v_{n1} \\ v_{12} & v_{22} & .. & v_{n2} \\ \vdots & \vdots & \vdots & \vdots \\ v_{1,(2n+2)} & v_{2,(2n+2)} & .. & v_{n,(2n+2)} \end{pmatrix} . \begin{pmatrix} r_1 \\ r_2 \\ \vdots \\ r_n \end{pmatrix} \tag{6}$$

Equation (6) applies analogously to the total acceleration at an element boundary.

In most cases of oscillation investigations, not all modes of a component are important. Modes which are hardly excited during operation and which hardly contribute to the static deformation can be neglected in order to reach a certain simplification, e.g.:

$$\begin{pmatrix} x_1 \\ x_2 \\ \vdots \\ x_{(2n+2)} \end{pmatrix} \approx \begin{pmatrix} v_{11} & v_{21} \\ v_{12} & v_{22} \\ \vdots & \vdots \\ v_{1(2n+2)} & v_{2(2n+2)} \end{pmatrix} . \begin{pmatrix} r_1 \\ r_2 \end{pmatrix} \tag{7}$$

This idea of modal condensation simplifies the system of equations of motion in Equation (5) ; e.g. neglecting all but the first two modes reduces the number of equations to two:

$$M_j\ddot{r}_j(t)+K_j\dot{r}_j(t)+S_j r_j(t)=p_j(t) \quad ; \quad j=1,2 \tag{8}$$

6.1.2 State-Space Estimators for Load Estimation

The suggested load estimation methodologies for vibratory components all involve one basic tool, which is the Luenberger Observer. Its principle will be shortly introduced.

If the real system to be observed can be considered linear and time invariant (e.g. by linearisation), it can be modelled as the state-space system:

$$\begin{aligned} \dot{z} &= \boldsymbol{A}\cdot z+\boldsymbol{B}\cdot u \\ y &= \boldsymbol{C}\cdot z+\boldsymbol{D}\cdot u \end{aligned} \tag{9}$$

$\boldsymbol{A}$ is an (*n,n*) matrix, the system output *y* represents a continuously measured quantity.

This model forms a part of the Luenberger observer, running parallel to the real system and being fed with the same input as the real system. In order to reach a continuous correction, a correction term is fed back into the model as additional input λ, which is the difference between

the measured real system output and the respective model output, multiplied with the observer gain matrix ***L***:

$$\boldsymbol{\lambda} = \boldsymbol{L} \cdot (y - \hat{y}) \tag{10}$$

Figure 6 contains the schematic of a Luenberger observer (bottom) in parallel to the real system to be observed (top). The quantity of interest x_i, i.e. the one to be estimated, is accessible in the model and can be read as output value. Its real trajectory can be traced - after a transient effect has decayed -, even if the initial conditions are not included in the model.

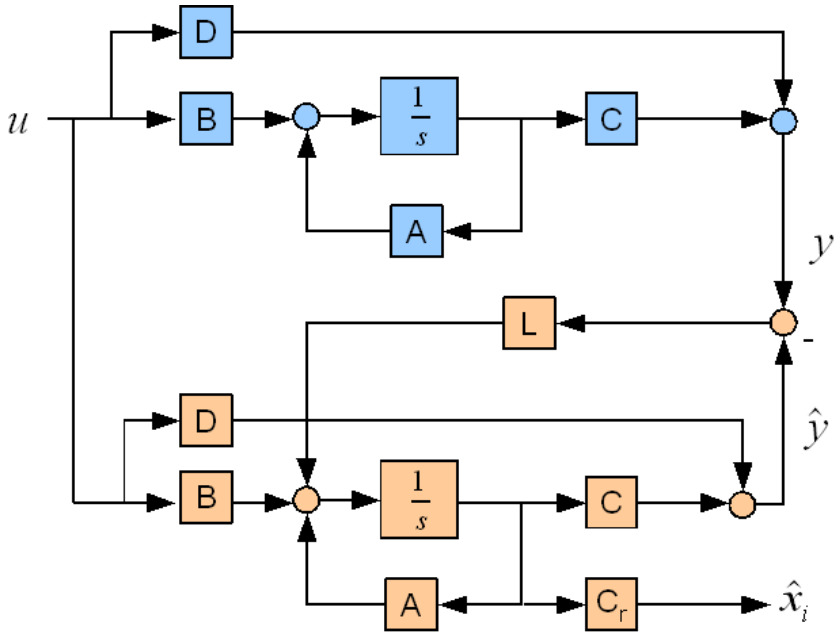

Figure 7: *Schematic of a Luenberger Observer (Bottom) in Parallel to the Real System to be Observed (Top)*
Fed with the same input as the real system and a correction feedback via the matrix L, the observer can reconstruct the real system's behaviour.

The general precondition for the application of this observation method is that the system ***(A, C)*** be observable. Observability is ensured, if the observability matrix $\boldsymbol{S_o}$ possesses maximum rank (Kalman criteria):

$$rank(\boldsymbol{S}_o) = rank\left(\begin{pmatrix} \boldsymbol{C} \\ \boldsymbol{C}\,\boldsymbol{A} \\ \boldsymbol{C}\,\boldsymbol{A}^2 \\ \vdots \\ \boldsymbol{C}\,\boldsymbol{A}^{(n-1)} \end{pmatrix}\right) = n \tag{11}$$

To allow for the observation error to converge to zero, the matrix ***L*** has to be designed such that the eigenvalues of the matrix ***A-LC*** possess negative real parts. Furthermore, to make the observation error die out quicker than the system's transfer behaviour, the eigenvalues have to be located clearly left from those of the matrix ***A***.

For the design of ***L***, since the eigenvalues of ***A-LC*** equal those of the matrix $\boldsymbol{A^T - C^T L^T}$, the system $\boldsymbol{(A^T, C^T)}$ with a state feedback via the gain matrix $\boldsymbol{L^T}$ is regarded. Then, $\boldsymbol{L^T}$ can be designed according to the requirements by pole placement.

If a process is subject to deterministic disturbances which are not accessible, those can be included in the observer model using additional system states, producing an extended model. Then, their impact on the system is not only considered, but they can even be observed themselves. However, not only a suitable model has to be built, but also the system observability has to be maintained.

The Luenberger observer is a so-called asymptotic observer; the estimation error asymptotically becomes zero after single impulse disturbances. However, if the process is permanently exposed to stochastic disturbances, an asymptotic observation is no longer possible.
In such cases, the Kalman filter proves more suitable as estimation method. It is based on the same structure as the Luenberger observer, but a different method to design the gain matrix ***L*** is used. In contrast to the Luenberger observer, it does not aim at eliminating the observation error but at minimizing its mean value. Instead of observer it is thus denoted estimator. The method used to design ***L*** is based on solving a Matrix-Riccati-Equation, taking into account the stochastic characteristics of the disturbances.

Since the measurements carried out for load estimation are subject to permanent stochastic disturbances, the Kalman filter promises to be more suitable as load estimation method. The suggested approach for load estimation on vibratory wind turbine components is to apply this estimation method in combination with the considerations in Section 6.1. However, in the basic simulations documented in the following sections, such measurement noise was not taken into account and Luenberger observers were used.

For assessing the the performance of a designed estimator, the Bode diagram can be used. It allows to compare the transfer behaviour of the estimator to that of the real system, both with respect to the real system's input. Good estimation can be expected where both amplitude and phase of the estimator's bode plot match those of the real system. For assessment, the relevance of the regarded frequencies has to be considered as well, i.e. their share in the component oscillations during the system's operation.
Another way is to test an estimator within simulations at realistic wind conditions. The estimation error can be continuously recorded and used as a measure of estimation performance.

6.2 Tower Bending Load Estimation

As mentioned in Section 2.6, both singular extreme load cases and fatigue loads due to tower oscillations play an important role when it comes to tower axial bending. Thus, in order to consider flexural vibrations, the application of a state-space estimator will be suggested.
Two measurement signals mentioned in Section 3 and 4 can provide information on the tower oscillatory motion: Strain measurements at the tower foot and acceleration measurements at the tower top.
Generally, the two bending directions can be treated independently. The total load can be calculated by superposing the estimated directional loads.

6.2.1 Tower Load Estimation from Measured Tower Foot Strains

Both fibre bragg grating sensors and conventional strain gauges allow to continuously measure a material's deformation which results from internal loads. Measuring the deformation at a point allows to evaluate the existing internal loads (normal stresses and shear stresses) which cause these deformations. As for normal stresses, the deformation (tensile strain ε) and the internal load (tensile stress σ) at the point in questions are related by $\sigma = E \cdot \varepsilon$, where ***E*** is the

material's young's modulus. Similarly, the shear stresses τ and shear strains γ are proportional, namely $\tau = G \cdot \gamma$, with *G* the shear modulus of the material.

The tensile stress distribution at a cross section is directly related to the internal loads, i.e. the acting bending moment M_b and the normal forces F_n:

$$\sigma(z,t) = -\frac{M_b(t)}{I_y} \cdot z + \frac{F_n}{A} \tag{12}$$

Similarly, the shear stresses are related to the shear force F_s:

$$\tau(z,t) = \frac{F_s(t) \cdot S_y(z)}{I_y \cdot b(z)} = \frac{F_s(t)}{I_y \cdot b(z)} \int_z^{e_1} \zeta \, dA \tag{13}$$

with

y	bending axis
z	coordinate in the cross-section perpendicular to the bending axis with *z=0* for the bending axis
I_y	2nd degree axial moment of area with respect to the bending axis
S_y	static moment of the cross section element between *z* and the border at $z=e_1$

For measuring normal stresses, four sensors can be used, arranged symmetrically around the cross section centre. Shear stresses can be measured using four pairs of sensors in the same symmetrical arrangement. One sensor of each pair is directed +45° , the other -45° from the vertical. This measurement installation allows to calculate the total (shear and normal) stress situation at the cross section e.g. using a finite volume model. Besides, the measured signals can be verified against one another.

Partitioning the cross section into a suitable number of elements, the stresses could be evaluated and logged for each of these elements for long term evaluations, in particular for fault prediction purposes.
Due to the high influence of thrust force on the tower load (causing the bending moment), the tower foot is the most highly loaded segment of the tower. The evaluation of internal tower foot loads can thus serve as a measure for the total tower loads.

However, the mentioned installation of strain sensors in the tower foot can also help to estimate the load distribution over the whole tower length. Within the following considerations, the two existing load directions – axial and lateral direction – are treated independently from each other. Both the measured bending moment and shear forces first have to be apportioned to the two bending directions. Since the nacelle changes its azimuthal orientation according to the wind speed, the direction of bending (due to thrust or generator torque fluctuations) changes with respect to the tower. Thus the current rotor yaw position is required for apportioning.

Translating Equation (4) to the situation of tower bending, the internal forces and moments can be calculated for each tower element from the external force and the distributions of tower displacement and acceleration. These total distributions are a superposition of all modal distributions as stated in Equation (6). Neglecting the aerodynamic forces which attack directly at the tower, the force p_j on element *j* equals zero for all elements except for the tower top element. Assuming that only the a few modes are relevant for these distributions both in terms of frequency and mode shape, an accordingly reduced tower model can be used in connection with a state estimator (see Section 6.1).
For the case of axial bending, the thrust force attacking at the tower top is assumed to be the only cause, neglecting the axial tower top bending moment. A schematic of a suggested

estimation method is shown in Figure 7. The top part represents a real tower oscillating system, containing an infinite number of modes. The system outputs are the measured stresses at the tower foot or, adequately, the tower foot bending moment. The state estimator is presented in the bottom part of the figure. It contains the simplified tower model, only taking into account e.g. the first two modes. The causing thrust force is contained in the estimator model as a disturbance state, modelled in step form. This enables the state estimator to estimate the current thrust force at the tower top, i.e. no thrust force input is required. The estimator correction feedback contains the difference between the measured and the estimated dynamic tower foot bending moment, multiplied by the state estimator gain vector ***L***. Since all system states are accessible, the thrust force and both the first and the second modal acceleration and deflection can be read as output values. Superposition according to Equation (6) leads to the estimated total distributions of deflection and acceleration.

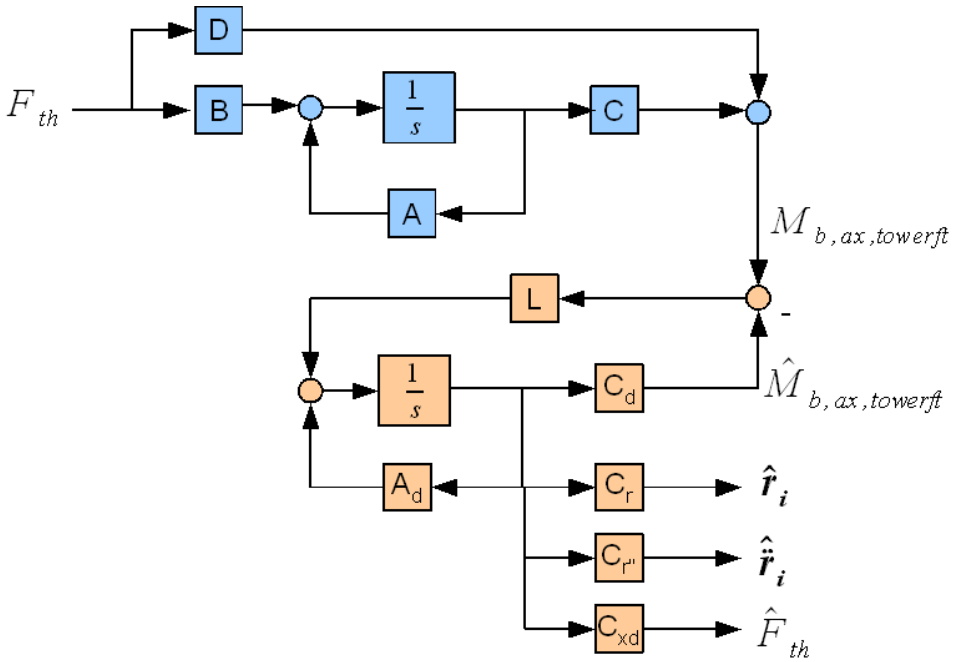

Figure 8: *Schematic of a Method to Estimate the Tower Deflection and Acceleration Using Strain Measurements at the Tower Foot*
The thrust force is considered via a step disturbance model and can be estimated as well as the system modal deflection and acceleration.

An exemplar three-mode tower model was used to design an estimator and to test the estimator performance by means of simulations. In order to test the effect of modal condensation, the estimator tower model is equipped only with the first two modes. The thrust force input is considered in form of a step disturbance model. Figure 8 contains a bode plot of the designed estimator in comparison to that of the 3-mode tower model. The real and the estimated tower top deflection are given both as response to the same tower thrust force input. A good match is resulting for static and low-frequent thrust force components, as well for the first mode frequency. Starting from there, neither the amplitude nor the phase don't fit satisfactorily. Only at the second eigen-frequency the two diagrams approach each other.
Figure 10 shows the simulated performance for turbulent wind conditions, comparing the real tower top deflection to the estimated course. Since the first mode oscillation the static component are decisive for the simulated tower top motion, the estimated course well matches the “real” course.

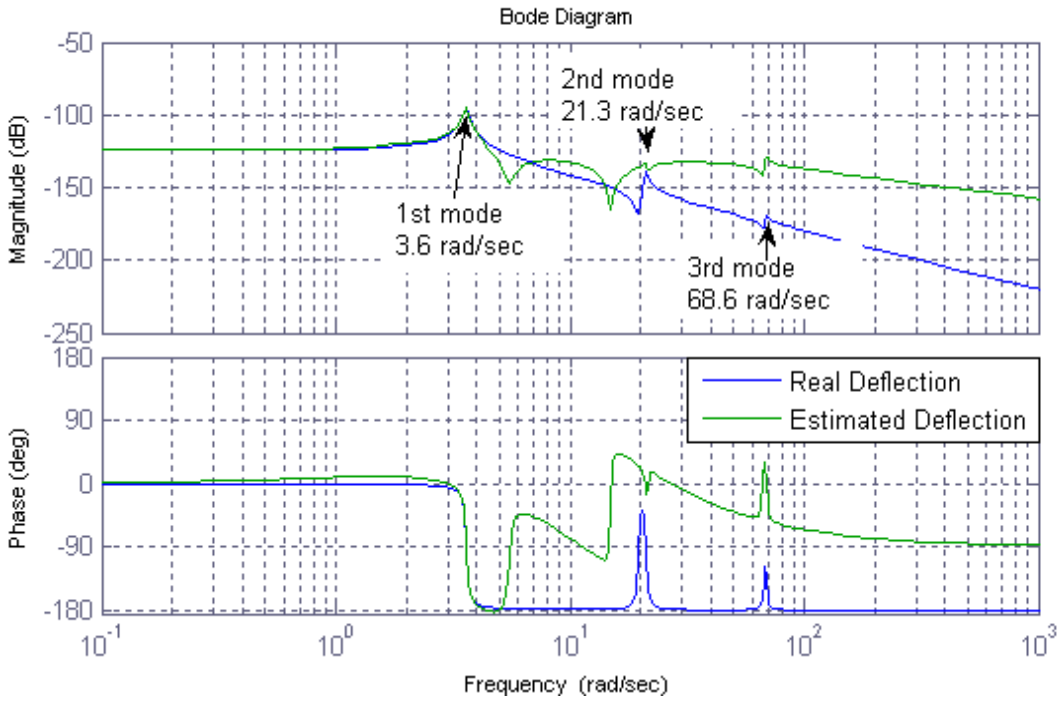

Figure 9: *Bode Diagrams for the 3-mode Tower Model (Force Input to Real Tower Top Deflection) and 2-mode Estimator (Force Input to Estimated Deflection)*

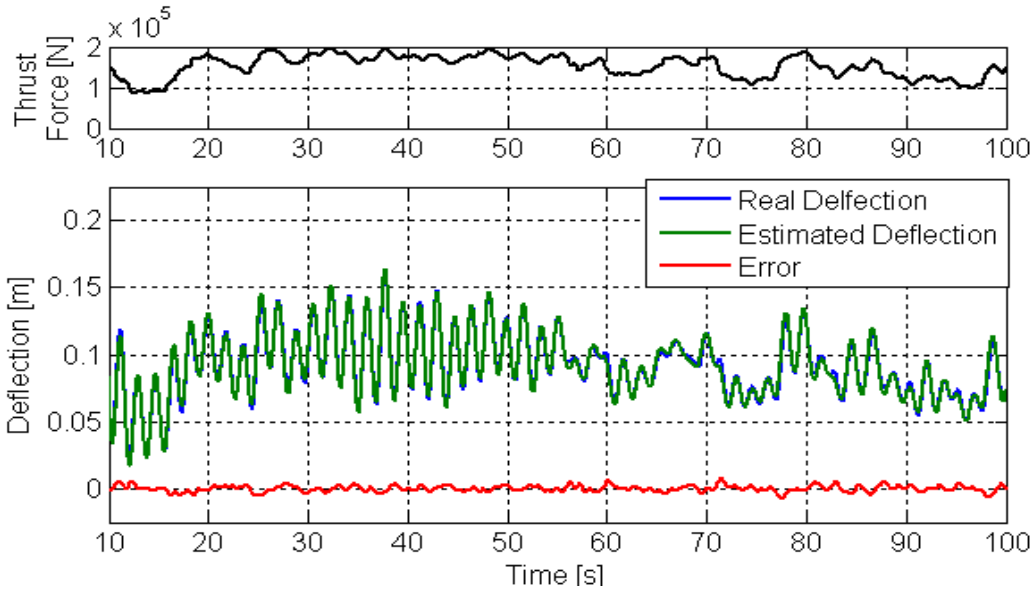

Figure 10: *Performance of the Estimation Method Shown in Figure 7 at Turbulent Wind Conditions*

The real tower model is equipped with the first three bending modes, the estimator with the first two modes and a step disturbance model to consider the thrust force input. The measured and estimated deflections are given for the tower top element.

The moment attacking at the tower top due to rotor gravity can be considered additionally in the estimator model as a known input. In order to take into account the stochastic rotor tilt moment, the measured tower foot shear force would have to be included in the estimation process as a second measurement.

For lateral tower bending, a similar estimation approach is promising. The model has to be built according to the modes which are relevant for lateral bending. The causing moment only attacks at the tower top and could as well be modelled as a disturbance.

Improvements could be reached by extending the state-space estimator and including a drive train model, incorporating generator speed and pitch angle measurements to advance wind speed estimation.

6.2.2 Tower Load Estimation from Tower Top Acceleration Sensor

Another way to estimate tower internal loads over the whole tower length is based on measurements of the tower top acceleration. This signal is more likely to be available in wind turbines than strain measurements. The approach is based on the considerations in Section 6. Again, the axial and the lateral load directions are treated separately.
As in Section 6.2.1, the ideas of modal analysis and condensation are used. Again, a state estimator is designed, containing a modally condensed model of the tower. A schematic is shown in Figure 11. The correction feedback is the difference between estimated and measured tower top acceleration, multiplied by the gain matrix $\boldsymbol{L}$. The tower modal deflections and accelerations for the modes contained in the estimator model are available as estimation output. Again, applying equation (6), the distributions of deflection and acceleration can be calculated for the whole tower.
In this case, the thrust force can not be included into the model as a disturbance state, because the system would lose its observability in this case. The state estimator is not able to estimate the thrust force from the measured acceleration. It is thus necessary to provide the thrust force to the state estimator as an input value. This quantity could be estimated with a certain delay using the method introduced in [10], see Section 5. Due to a smoothing effect, short term thrust force fluctuations are not contained. However, the impact of deterministic fluctuations e.g. due to the tower shadow effect and wind shear can be estimated by means of disturbance modelling. The estimator could thus equipped with a sinusoidal disturbance model representing the thrust force component at a given frequency of 3p. The frequency variation with rotor speed provokes that the disturbance model frequency has to be chosen according to the rotor speed. Thus, both the model and the gain vector $\boldsymbol{L}$ are subject to scheduling.

An exemplar three-mode tower model was used to design an estimator and to test the estimator performance by means of simulations. The estimator is equipped with the two first bending modes and a disturbance model at a frequency of 0.85 Hz. The gain matrix $\boldsymbol{L}$ was designed by means of pole placement. The thrust force input to the estimator is simply modelled by applying a filter on the real thrust force signal. Further, no gain scheduling is taken into account; disturbance frequencies are modelled as constants.

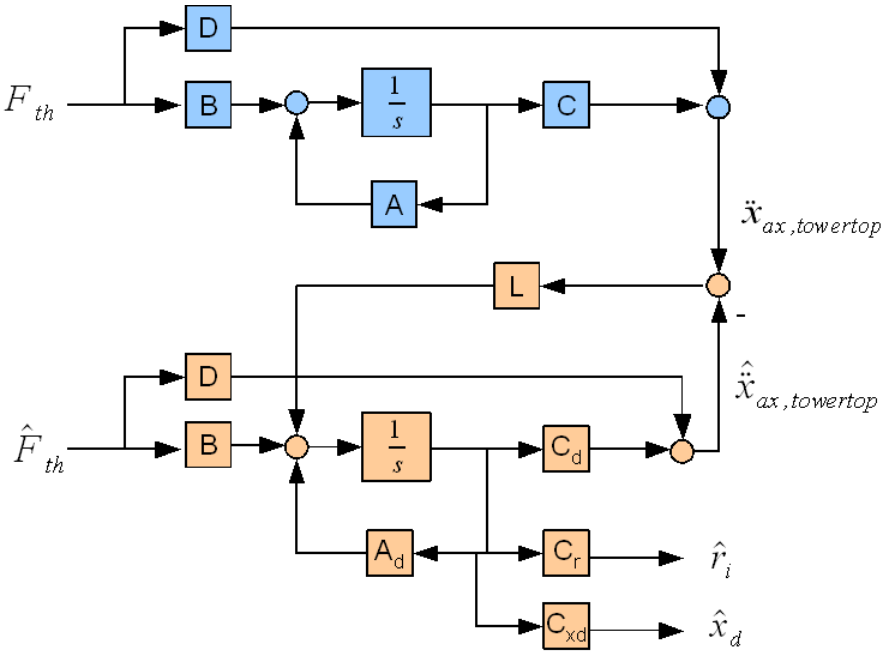

Figure 11: *Schematic of a Method to Estimate the Tower Deflection and Acceleration Using an Acceleration Measurement at the Tower Top*
The static thrust force component can e.g. be provided to the estimator by a separate estimation system introduced in [10].

Figure 12 shows a Bode diagram of the real system's transfer function (real thrust force to real deflection) in comparison to the estimator system's transfer function (real thrust force to estimated deflection). Static and low frequent oscillations are well estimated thanks to the thrust force input to the estimator. Also, for the first and second mode oscillations the method promises good estimation results. The same is true for oscillations at the modelled disturbance frequency. However, aside of these frequencies, both the amplitudes and the phases of the two transfer functions differ considerably from each other. While oscillations at frequencies around 1.5 rad/sec are underestimated, those beyond the second mode frequency are overestimated by far.

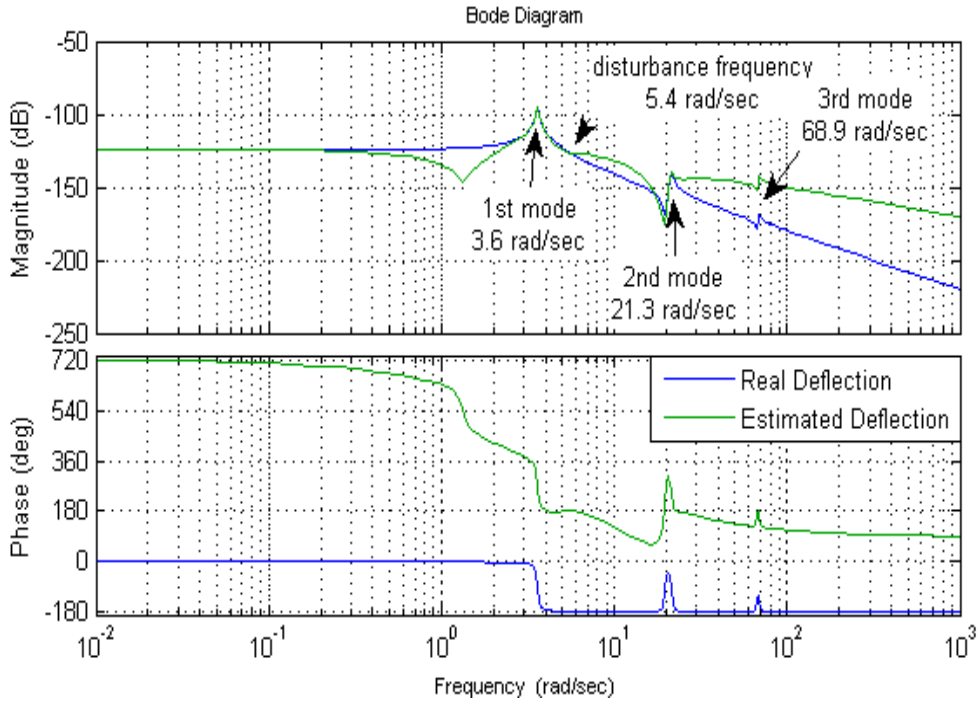

Figure 12: *Bode Diagrams for the 3-mode Tower Model (Real Force Input to Real Tower Top Deflection) and 2-mode Estimator Fed with Static Thrust Force (Real Force Input to Estimated Deflection)*

Figure 13 compares the tower top deflection of the “real” tower model with the estimated values for turbulent wind conditions and a sinusoidal thrust force component at the modelled disturbance frequency. While the estimator shows a satisfactory performance for the long-term static component and the sinusoidal oscillations, estimation errors occur at thrust force steps.

The axial tower top bending moment is not considered in modelled estimator. However, the moment due to gravity can be included as a constant input, since it is known. As for the tilt moment, its deterministic sinusoidal components at known frequencies could be included as disturbances.

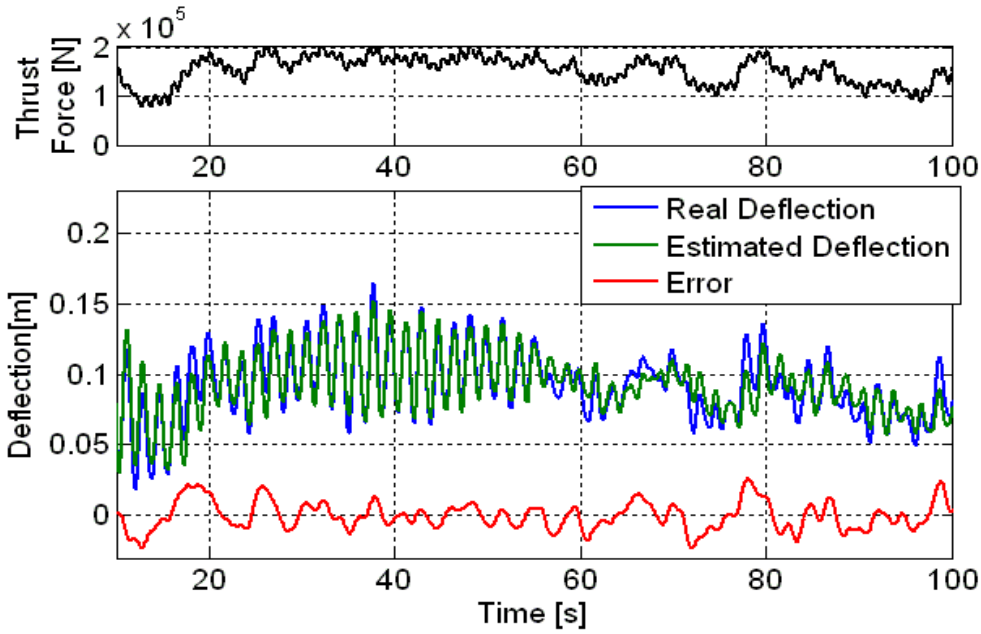

Figure 13: *Performance of the Estimation Method Shown in Figure 12 at Turbulent Wind Conditions and a Sinusoidal Thrust Force Component at 3p*
The static thrust force component is provided to the estimator by means of filtering the real signal with time constant 2 sec. The "real" tower model considers three modes, the estimator is equipped with two modes and a disturbance model at 3p frequency.

An alternative to retrieve the thrust force value from a separate estimation could be to extend the state-space estimator and include a drive train model, incorporating generator speed and pitch angle measurements. The uniform wind speed could then be modelled as a step disturbance, which allows to simultaneously estimate the rotor thrust force.

6.3 Blade Load Estimation

As stated in Section 2.1, the blade loads consist of several components. The most important components are:

- blade in-plane bending stresses due to gravity and tangential aerodynamic forces
- blade out-of-plane bending stresses due to axial aerodynamic forces
- blade bending stresses due to flapwise and edgewise natural oscillations
- radial stresses due to gravity and centrifugal forces
- torsional shear stresses due to aerodynamic forces and pitch action

In order to deal with a blade-based coordinate system, all in-plane and out-of-plane loads can be converted into the edgewise/flapwise system, using the current angle θ, see Figure 2.

Similar to the tower foot, the blade root has to stand the highest internal loads in the blade. This is due to the fact that both bending moment and radial forces reach their highest values at the blade root. The blade root loads can thus serve as a measure for the total blade loading. Besides, if the blade root bending moments are measured or properly estimated, the rotor yaw and tilt moment can be reconstructed. This in turn allows to detect related loads on the main shaft, on the drive train bearings, the yawing unit and on the tower.
However, the internal load distribution over the whole blade is as well an interesting estimation aim, especially for blade condition monitoring.

A simplified load estimation can be carried out involving most load components, neglecting the impact of structural oscillations and short term fluctuations of local aerodynamic forces. This simple method does not require measurements at the blade. A more detailed estimation promises to be difficult with the considered measurement signals. A state-space estimator is suggested, which could work either with a blade root strain measurement signal or a blade acceleration signal. However, certain simplifying assumptions are necessary for this method to be applied for blade load estimation.

6.3.1 Simplified Blade Loads Estimation from Rotor Speed and Position, Generator Speed and Power Output

Several components of the blade root loads can be estimated using an quasi-static physical model. However, this implies neglecting short term load fluctuations e.g. due to blade structural oscillations or fluctuations of aerodynamic forces.
Using the rotor position signal and the rotor speed, it is possible to estimate

- dynamic radial stresses due to gravity
- dynamic radial stresses due to centrifugal forces
- dynamic blade in-plane bending stresses due to gravity

Further, by applying the estimation method introduced in [10], two other important components can be estimated:

- dynamic blade in-plane bending stresses due to aerodynamic torque, averaged over the three blades
- blade out-of-plane bending stresses due to aerodynamic thrust, averaged over the three blades

Radial stresses at the blade root can be estimated continuously knowing the current blade position on the rotor surface, which is determined by the angle φ_i as shown in Figure 14. The radial force acting at the blade root due to gravity can be calculated using

$$F_{rad,gr,i} = -M_{bl} \cdot g \cdot \cos(\varphi_i(t)) \tag{14}$$

where

M_{bl} absolute blade mass
g acceleration of gravity

Negative values stand for a compressive force and positive values stand for a tensile force at the blade root. Similarly, the radial centrifugal forces can be evaluated by

$$F_{rad,cen,i} = \omega^2(t) \cdot \int_0^R m_{bl}(r) \cdot r \, dr \tag{15}$$

where

ω rotor speed
m_{bl} relative blade mass per unit length
r coordinate along the blade radius, $r=0$ at the hub axis
R Blade length

With a uniform force distribution on the blade root, the radial compressive and tensile stresses due to gravity and centrifugal forces can be determined using

$$\sigma_{rad,grav+cen,i} = \frac{F_{rad,gr,i}(t) + F_{rad,cen,i}(t)}{A_{root}} \tag{16}$$

where
A_{root} blade root cross section

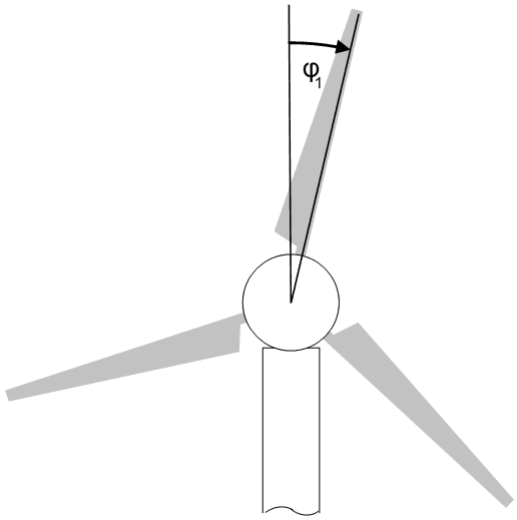

Figure 14: *Definition of Angle φ to Describe the Blade Position in the Rotor Plane*

The in-plane bending moment and the transverse force at the root of blade *i* due to gravitational forces can be calculated with Equation (17) and (18).

$$M_{ip,gr,i}(t) = \int_0^R m_{bl}(r) \cdot r \, dr \cdot g \cdot \sin(\varphi_i(t)) \tag{17}$$

$$F_{ip,gr,i}(t) = \int_0^R m_{bl}(r) dr \cdot g \cdot \sin(\varphi_i(t)) \tag{18}$$

The rotor aerodynamic torque is produced by the three blades, which experience both an according in-plane- blade root bending moment and an in-plane shear force. Since the blade root is not located directly at the hub axis, the shear forces contribute to the aerodynamic torque:

$$T_{aero} = \sum_{i=1}^{3} M_{ip,trq,i} + \sum_{i=1}^{3} F_{ip,trq,i} \cdot r_{bladert} \tag{19}$$

If inhomogeneity of the wind field is neglected, a substitutional point of attack for the tangential aerodynamic forces, $r(S_{trq})$, can be assumed to be known for each operation point from the blade characteristics. Simplistically assuming further that the aerodynamic torque is produced by the three blades in equal shares, the in-plane-bending moment due to the aerodynamic torque is:

$$M_{ip,trq,i}(t)=\frac{T_{aero}(t)}{3\cdot\left(1+\frac{r_{bladert}}{r(S_{trq})}\right)} \tag{20}$$

The aerodynamic torque is calculable from the generator speed and generator electrical power signal, knowing the drive train efficiency and inertia, see [10]. The according transverse force is then

$$F_{ip,trq,i}(t)=\frac{M_{ip,trq,i}(t)}{r(S_{trq})} \tag{21}$$

Similar to S_{trq}, if a known constant distribution of thrust over the blade is assumed, a thrust force substitutional point of attack S_{thr} can be determined. Assuming that the aerodynamic thrust on the rotor is produced by the three blades in equal shares, the according out-of-plane blade root bending moment and the blade root thrust force is calculable as:

$$M_{oop,thr,i}(t)=\frac{F_{thr}(t)}{3}\cdot r(S_{thr}) \tag{22}$$

$$F_{oop,thr,i}(t)=\frac{F_{thr}(t)}{3} \tag{23}$$

The thrust on the rotor can be calculated via the aerodynamic torque, using the pitch angle and knowing the according aerodynamic coefficients of the blades, as introduced in [10].

The in-plane bending normal stresses and shear stresses due to gravity and tangential aerodynamic forces which result from these estimations can finally be calculated using:

$$\sigma_{b,ip,i}(z,t)=-\frac{M_{ip,i}(t)}{I_y}\cdot z=-\frac{M_{ip,gr,i}(t)+M_{ip,trq,i}(t)}{\int z^2\,dA_{root}}\cdot z \tag{24}$$

$$\tau_{ip,i}(z,t)=\frac{F_{ip,i}(t)\cdot S_y(z)}{I_y\cdot b(z)}=\frac{F_{ip,i}(t)}{I_y\cdot b(z)}\int_z^{e_1}\zeta\,dA \tag{25}$$

where

z	coordinate in in-plane-direction perpendicular to the bending axis (y-axis)
I_y	blade root's moment of area with respect to the bending axis y
$S_y(z)$	static moment of the cross section element between z and the border at $z=e_1$

The normal and shear stresses which are caused by the aerodynamic thrust force can be calculated analogously from the estimations from Equations (22) and (23).

In case the estimated loads are used for long-term evaluations such as health monitoring or fault prediction, they have to be translated into the blade-based edgewise/flapwise system. This transformation is carried out using the angle θ, see Figure 2. Using a finite volume model of the blade root cross section, the estimated internal loads could be calculated and stored for each element.

Using the same estimation approach, also the loads could be estimated for each blade element over the radius. Again, for the cases of torque and thrust-related loads, an ideal uniform wind field has to be assumed. For this case, not only the three blades contribute equally to the torque and rotor thrust, but also the contribution of each blade element is given (provided that the distribution of torque and thrust coefficients are known). In contrast to the blade root case, the moment of area with respect to the in- and out-of-plane bending axis varies with the pitch angle for each element along the blade.

The documented method allows to well estimate the radial stresses, which arise due to centrifugal forces and gravity, since both centrifugal forces and gravity are well calculable. Errors will occur if the blade mass or its distribution change e.g. due to icing.
However, regarding the blade root bending loads, this method can only give a rough and static load estimate, which does not reflect the real situation, since several important load components are not taken into account. This includes the loads due to fluctuation of aerodynamic forces, e.g. forced oscillations induced by the tower shadow effect or stochastic bending loads due to stochastic wind speed variation. Additionally, loads resulting from blade natural oscillations are not considered.

Even if this method is not expected to serve as a useful tool for load mitigating control or for detailed load monitoring, it can give a rough estimate without additional sensors to be installed in the blade. It can also provide a verification of more advanced blade load estimation methods.

6.3.2 Estimation of Blade Loads from Strain Measurement at the Blade Root

Similar to Section 6.2.1, the blade root internal loads can be evaluated using strain sensors, such as fibre bragg grating sensors or conventional strain gauges.
Again, four sensors can be placed in the blade root for measuring the normal stresses, arranged symmetrically around the cross section centre. For shear stress measurement, four pairs of sensors in the same symmetrical arrangement can be used, one sensor of each pair being directed +45° , the other -45° from the vertical.
Figure 15 shows a schematic of an possible strain sensor arrangement in the blade root cross section. Obviously, the sensor positions with respect to the hub vary with the pitch angle.

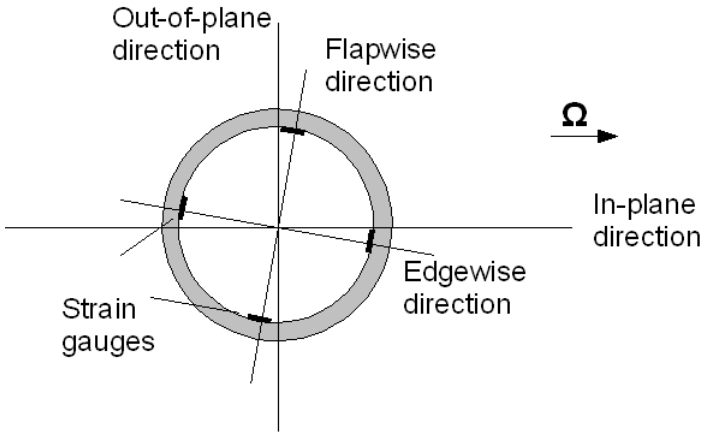

Figure 15: *Possible Sensor Arrangement for Strain Measurement at the Blade Root*

This measurement installation allows to calculate the total (shear and normal) stress situation at the cross section and a certain signal verification. Again, a finite volume model can be used for continuously calculating and recording the stresses on the whole blade root cross section. An additional verification can be carried out using the estimation method in Section 6.3.1.

If certain assumptions are made, the strain measurement at the blade root also allows to give estimates on the bending stress situation of the whole blade, involving a state-space estimator. In the following considerations, the two blade bending directions – flapwise and edgewise – are not treated independently from each other as done for the tower. A separation would be complicated by the fact that the directions vary along the blade due to the blade twist:
Flapwise bending is caused by all forces along the blade radius which act in the *local* flapwise direction. Those include the flapwise components of both aerodynamic forces and of gravity. In turn, the residual edgewise components of both aerodynamic forces and gravity cause edgewise bending. Due to the twist, the measured local shear force and bending moment direction due to flapwise bending does not coincide with the local flapwise direction (which is orthogonal to the local weak principal axis). Thus, the blade motion is modelled two-dimensionally.

The blade root bending moment is described by:

$$\vec{M}_{b,bladert}(t)=\int_0^R \vec{f}_{aero}(t)\times\vec{r}\,dr+\int_0^R \vec{f}_{grav}(t)\times\vec{r}\,dr-\int_0^R m(r)\cdot\ddot{\vec{x}}(r,t)\times\vec{r}\,dr \tag{26}$$

The shear force which results from flapwise forces along the blade is:

$$\vec{F}_{shear,bladert}(t)=\int_0^R \vec{f}_{aero}(t)\,dr+\int_0^R \vec{f}_{grav}(t)\,dr-\int_0^R m(r)\cdot\ddot{\vec{x}}(r,t)\,dr \tag{27}$$

Applying Equation (4) on the blade bending situation shows, that in order to estimate the internal load situation for an element *j*, it is necessary to know both the displacement and shear angle including the respective accelerations as well as the external force and moment at the element boundaries.

In order to estimate the distributions of deflection and acceleration using strain measurements at the blade root, the method introduced in Section 6.1 can be used as a basis. However, the situation is more complex than for the tower bending, since the causing force does not attack at a defined point but is distributed over the whole blade.
In a first step, the relative distribution of aerodynamic forces $\vec{\boldsymbol{d}}_{\boldsymbol{aero}}$ on the blade is assumed to be known. This means, a relative distribution of relative wind speed along the blade is assumed, the deviations from this distribution are neglected. The assumed distributions $\vec{\boldsymbol{d}}_{\boldsymbol{aero}}$ can vary e.g. with the operation point or wind conditions. The aerodynamic force distribution can then be described by Equation (28).

$$\vec{\boldsymbol{F}}_{\boldsymbol{aero}}(t)=F_{aero}(t)\cdot\vec{\boldsymbol{d}}_{\boldsymbol{aero}}=F_{aero}(t)\cdot\begin{pmatrix}\vec{d}_{aero,1}\\ \vec{d}_{aero,2}\\ \vdots\\ \vec{d}_{aero,n}\end{pmatrix} \tag{28}$$

The blade root bending moment can be described in discrete form by:

$$\vec{M}_{b,bladert}(t)=F_{aero}(t)\cdot\sum_{i=1}^{n}\vec{d}_{aero,i}\times\vec{r}_i+\sum_{i=1}^{n}\vec{f}_{grav,i}(t)\times\vec{r}_i-\sum_{i=1}^{n}M_i\cdot\ddot{\vec{x}}_i(t)\times\vec{r}_i \tag{29}$$

Analogously, the shear force at the blade root due to flapwise forces is:

$$\vec{F}_{shear,bladert}(t) = F_{aero}(t) \cdot \sum_{i=1}^{n} \vec{d}_{aero,i} + \sum_{i=1}^{n} \vec{f}_{grav,i}(t) - \sum_{i=1}^{n} M_i \cdot \ddot{\vec{x}}_i(t) \tag{30}$$

For the blade load estimation, a state estimator is suggested which contains a two-dimensional blade oscillation model, similar Section 6.2.1. Using modal condensation, only the relevant (in terms of frequency and mode shape) modes should be included. The two-dimensional blade root bending moment which is retrieved from the blade root strain measurements, serves as correction input for the estimator. Furthermore, information on the force distribution input to the state estimator is necessary. The share which results from gravity, $\vec{F}_{grav}$ can be continuously calculated from the rotor position, pitch angle, blade twist and mass distribution. The aerodynamic force distribution $\vec{F}_{aero}$ could possibly be estimated by implementing a step disturbance model for the scalar F_{aero} in the state estimator, as similarly done in Section 6.2.1. The schematic of this estimation method is analogue to that shown in Figure 7.
Another way to consider $\vec{F}_{aero}$ is to estimate its static value separately and to use it as an input for the state estimator. For this, the measured shear force in Equation (30) can be filtered in order to eliminate the inert force component. The "static" force distribution can then be estimated according to Equation (31):

$$\vec{F}(t) = \vec{F}_{aero}(t) + \vec{F}_{grav}(t) = \frac{\vec{F}_{shear,bladert,fil}(t) - \sum_{i=1}^{n} \vec{f}_{grav,i}(t)}{\sum_{i=1}^{n} \vec{d}_{aero,i}} \cdot \vec{d}_{aero} + \vec{F}_{grav}(t) \tag{31}$$

Similarly, Equation (29) can be applied to the filtered measured blade root bending moment as in Equation (32). The filter has to be designed such that the inert force components in Equation (29) are eliminated.

$$\vec{F}(t) = \frac{\vec{M}_{b,bladert,fil}(t) - \sum_{i=1}^{n} \vec{f}_{grav,i}(t) \times \vec{r}_i}{\sum_{i=1}^{n} \vec{d}_{aero,i} \times \vec{r}_i} \cdot \vec{d}_{aero} + \vec{F}_{grav}(t) \tag{32}$$

Note that each of these variants depends on a known relative distribution of aerodynamic forces.

Figure 16 shows a schematic of the latter estimation variant. The tower flapwise bending model is contained in the top part, with the measured resulting blade root bending moment as system output. Apart from the state estimator, a step is included to provide the estimated force distribution acting along the blade radius (bottom). Due to the filter, the force distribution provided to the state estimator would lack short term force fluctuations above certain frequencies. The resulting forced oscillations can not be retraced by the estimator. However, the estimator can be enabled to consider forced oscillations at deterministic, known frequencies by including the according force fluctuations in the state estimator as disturbances.

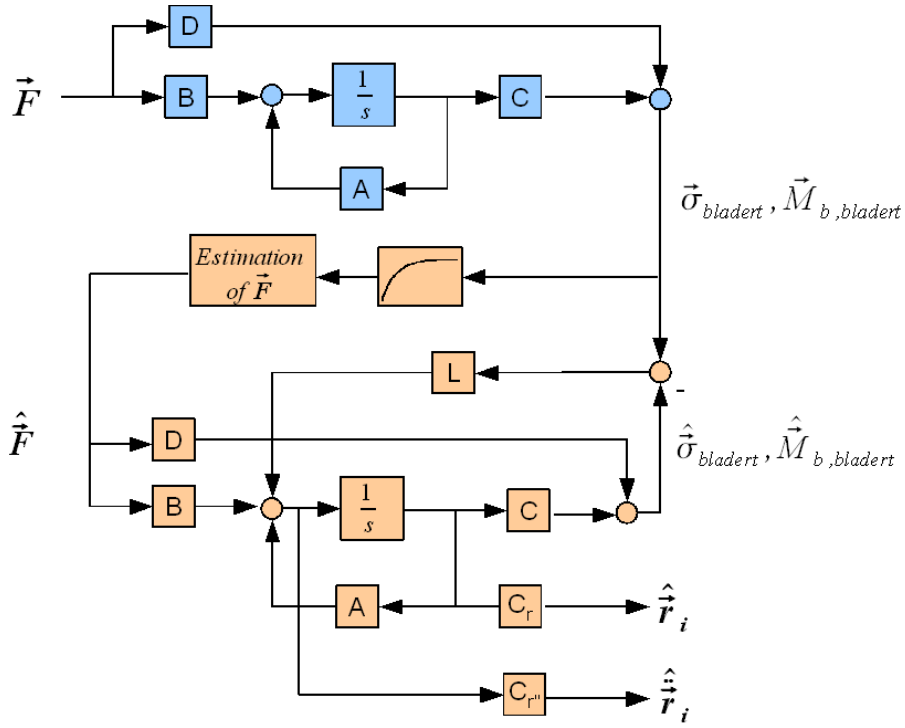

Figure 16: *Schematic of a Method to Estimate the Blade Deflection and Acceleration Using Strain Measurements at the Blade Root*
The real blade oscillation system is contained in the top, the estimator in the bottom. The method requires a known relative distribution of forces acting along the blade radius.

This method can in principal be expected to estimate both the distribution of deflection and acceleration at blade natural oscillations and forced oscillations which are contained in the state estimator model, including static components. Together with the estimated total force distribution, the blade bending load distribution can be calculated using Equation (4).

However, the estimation method performance depends strongly on the impact of assuming a known force distribution over the blade.

Improvements to this method could be expected if strain measurements were carried out at several cross sections along the blade and involved in the estimation process. However, in order to be able to actually estimate the aerodynamic force distribution (without the need to assume a relative distribution), each blade element to be regarded would have to be equipped with its own strain measurement.

6.3.3 From acceleration sensors in the blade

Another signal which can be used for estimating the blade bending loads is the acceleration measured at a defined location of the blade. Again, the blade bending directions – flapwise and edgewise – are treated together, using a two-dimensional model. At radius l_m, two acceleration sensors are placed in the blade cross section: one to measure flapwise acceleration, the other one to measure edgewise acceleration. l_m has to be chosen such that it does not match the nodes of the most important modes.
As in Section 6.3.2, the relative aerodynamic force distribution along the blade radius is assumed to be known.

Similar to the method introduced in Section 6.2.2, the state estimator approach is proposed to estimate the internal blade load distribution, see Section 6.1. By means of modal analysis and modal condensation, a reduced model can be developed for blade bending respectively, containing only a small number of modes.
For bending load estimation, the measured acceleration vector could be used as correction input to the filter. Furthermore, a static force distribution input is required. While the gravity-related component can be calculated continuously from the rotor position, the pitch angle and the blade's mass distribution, the aerodynamic component has to be estimated.
This can be done assuming a known relative distribution:
As stated before, the aerodynamic forces acting in flapwise and in edgewise direction on a blade element are related to the respective in-plane and out-of-plane force components according to Equations (33):

$$\vec{f}_{aero,i}(t)=\vec{f}_{aero,oop,i}(t)+\vec{f}_{aero,ip,i}(t) \tag{33}$$

While the in-plane aerodynamic forces over all blade elements form the rotor aerodynamic torque, the out-of-plane aerodynamic forces result in the aerodynamic thrust on the three-bladed rotor:

$$\begin{aligned}\vec{T}_{aero}(t)&=\sum_{j=1}^{3}\sum_{i=1}^{n}\vec{f}_{aero,i,j}(t)\times\vec{r}(i,j)=F_{aero}\cdot\sum_{j=1}^{3}\sum_{i=1}^{n}\vec{d}_{aero,i,j}(t)\times\vec{r}(i,j)\\ \vec{F}_{th,aero}(t)&=\sum_{j=1}^{3}\sum_{i=1}^{n}\vec{f}_{aero,i,j}(t)\cdot\vec{e}_{oop}=F_{aero}\cdot\sum_{j=1}^{3}\sum_{i=1}^{n}\vec{d}_{aero,i,j}(t)\cdot\vec{e}_{oop}\end{aligned} \tag{34}$$

where

$\vec{e}_{oop}$ unit vector in out-of-plane direction

Both the aerodynamic torque and thrust can be estimated e.g. using the method introduced in [10] or from a state estimator for the drive train loads, see Section 6.5. Using the assumption of a known relative force distribution not only among blade elements (as stated before) but also among the blades, the static value of aerodynamic flapwise forces can be estimated by applying Equations (33) and (35):

$$\begin{aligned}\vec{f}_{aero,i,j}(t)&=F_{aero}\cdot\vec{d}_{i,j}(t)=\frac{\vec{T}_{aero}(t)}{\sum_{j=1}^{3}\sum_{i=1}^{n}\vec{d}_{aero,i,j}(t)\times\vec{r}(i,j)}\cdot\vec{d}_{aero,i,j}(t)\\ \vec{f}_{aero,i,j}(t)&=F_{aero}\cdot\vec{d}_{i,j}(t)=\frac{\vec{F}_{th,aero}(t)}{\sum_{j=1}^{3}\sum_{i=1}^{n}\vec{d}_{i,j}(t)}\cdot\vec{d}_{i,j}(t)\end{aligned} \tag{35}$$

With this method, only the static component of aerodynamic forces can be estimated, because aerodynamic thrust and torque estimation is subject to some time delay and short time-fluctuations are smoothed. Deterministic effects such as the wind shear could potentially be considered by adapting the relative force distribution among the blade elements and the blades. Another way to include those effects is to implement a sinusoidal disturbance model into the state estimator as also proposed in Section 6.2.2. As an advantage, only the disturbance frequency is required, not its amplitude. Again, gain and model scheduling would be necessary, since the disturbance frequency depends on the rotor speed, equalling e.g. 1p in case of the wind shear effect. This feature might additionally allow to detect a yaw or tilt moment, see Section 6.4.

Figure 17 shows a schematic of the state estimator based estimation method for load estimation at blade *j*.

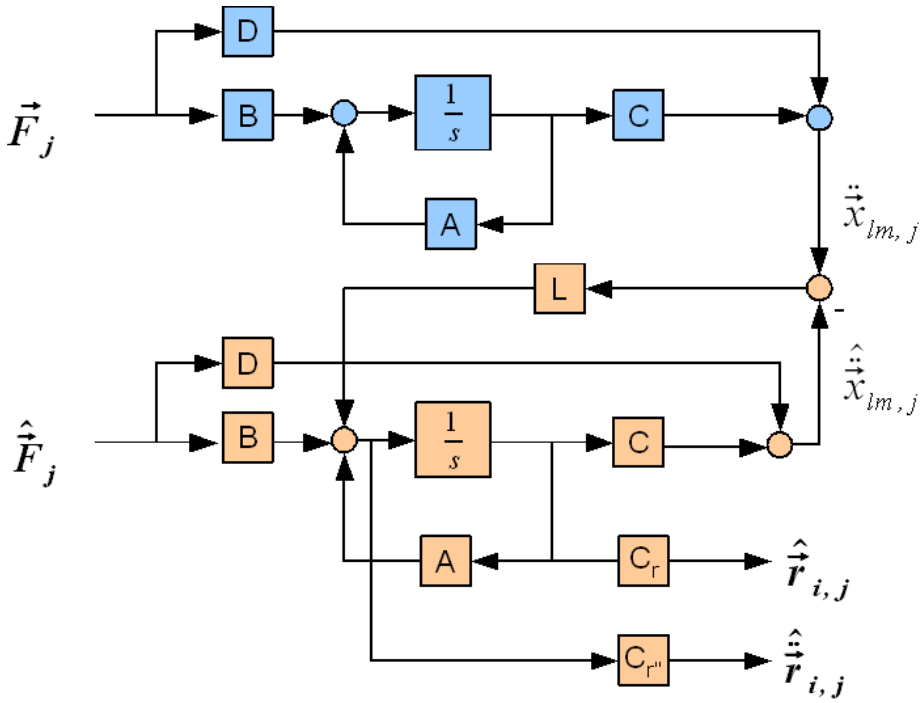

Figure 17: *Schematic of a Method to Estimate the Blade Flapwise Deflection and Acceleration Using the Measured Acceleration at an Element at Distance l_m to the Blade Root*
The real blade oscillation system is shown in the top, the estimator in the bottom part. The method requires a known relative distribution of forces along the blade radius and among the blades. The static force component has to be estimated additionally.

Improvements to this method can be expected if acceleration measurements were carried out at several cross sections along the blade and involved in the estimation process.

6.4 Yaw and Tilt Moment Estimation

Both the yaw and the tilt moment result from thrust force distributions on the rotor surface, which are unsymmetric with respect to the vertical rotor axis (in case of the yaw moment) or the horizontal in-plane rotor axis (tilt moment) respectively. They not only cause a dynamic bending load component on the blades but also interaction loads on other turbine components. Those include bending loads on the main shaft and axial bending (in case of a tilt moment) and torsional load (in case of a yaw moment) on the tower. Thus, estimating the yaw and tilt moment allows to reconstruct several interaction loads on other turbine components.

Both yaw and tilt moments are directly related to the out-of-plane components of the three blade root bending moments and blade root shear forces. The total rotor moment can be calculated using:

$$\begin{aligned}\vec{M}_{b,yt}(t) &= \vec{M}_{b,oop,1}(t) + \vec{M}_{b,oop,2}(t) + \vec{M}_{b,oop,3}(t) \\ &= \sum_{j=1}^{3} \vec{M}_{b,oop,bladert,j}(t) + \vec{F}_{shear,oop,bladert,j}(t) \times \vec{d}_{bladert}\end{aligned} \tag{36}$$

where

$\vec{d}_{bladert}$ vector between rotor centre and blade root

The total rotor moment can be divided into its yaw and tilt components by

$$\begin{aligned}M_{b,yaw}(t) &= M_{b,yt}(t) \cdot \cos(\varphi_{Mb,yt}(t)) \\ M_{b,tilt}(t) &= M_{b,yt}(t) \cdot \sin(\varphi_{Mb,yt}(t))\end{aligned} \tag{37}$$

Both the blade root out-of-plane bending moments and shear forces could be calculated from blade root strain measurements as proposed in Section 6.3.2. In case this measurement installation is not available, the magnitudes could be estimated using the method introduced in Section 6.3.3, where a disturbance at *1p* frequency has to be included in the sate-space estimator.

6.5 Main shaft torsional loads

During operation, the main shaft is permanently exposed to torsional loads. For a constant aerodynamic torque and constant generator torque, the torsional load is constant and homogeneous over the shaft's length. Dynamic loads occur if the torque, which is transmitted over the shaft, fluctuates. Such changes can be caused by changes of the aerodynamic torque (e.g. due to wind speed fluctuation or pitch action) or the generator torque. Drive train oscillations can be excited in such cases. In order to estimate the torsional load, a state-space estimator is thus suggested.

To describe a shaft element *j* loaded with torsion, the element displacement vector contains the local shear angles at the element boundaries: $\boldsymbol{u}_j^T(t) = \{\varphi_0(t), \varphi_1(t)\}_j$. Analogue to Equation (4), the cut load, i.e. the acting torque at the boundaries of the shaft element depends on the local twist angle and the local angular acceleration:

$$\boldsymbol{s}_j(t) = [-T_0(t) \quad T_1(t)]_j^T = \boldsymbol{S}_j \cdot \boldsymbol{u}_j(t) + \boldsymbol{\Phi}_j \cdot \ddot{\boldsymbol{u}}_j(t) - \boldsymbol{T}_j(t) \tag{38}$$

where

$\boldsymbol{S_j}$ element stiffness matrix
$\boldsymbol{\Phi_j}$ element inertia matrix
$\boldsymbol{T_j}$ external torque vector on element
$T_{0,1}$ local internal torque at element boundaries

The resulting local shear stresses within the shaft due to torsional load can be calculated from the local torque and the radius within the cross section:

$$\tau(r,t)_{sh,tors} = \frac{T(t)}{I_p} \cdot r = \frac{T(t)}{\int_0^R r^2 \, dA} \cdot r \tag{39}$$

where

I_p cross section polar moment of area

r radial distance of element dA from the cross section centre

The behaviour of a system performing torsional oscillations can be described with an equation of motion. It as well contains inertial, damping and stiffness characteristics of the system and uses the degrees of freedom as system states. For a drive train containing the three blades, the rotor hub and the generator, the discrete system of equations is, neglecting the damping:

$$\begin{pmatrix} \theta_1 & 0 & 0 & 0 & 0 \\ 0 & \theta_2 & 0 & 0 & 0 \\ 0 & 0 & \theta_3 & 0 & 0 \\ 0 & 0 & 0 & \theta_n & 0 \\ 0 & 0 & 0 & 0 & \theta_{gen} \end{pmatrix} \begin{pmatrix} \ddot{\varphi}_1 \\ \ddot{\varphi}_2 \\ \ddot{\varphi}_3 \\ \ddot{\varphi}_n \\ \ddot{\varphi}_{gen} \end{pmatrix} + \begin{pmatrix} s_1 & 0 & 0 & -s_1 & 0 \\ 0 & s_2 & 0 & -s_2 & 0 \\ 0 & 0 & s_3 & -s_3 & 0 \\ -s_1 & -s_2 & -s_3 & s_{sh} + \sum_{i=1}^{3} s_i & -s_{sh} \\ 0 & 0 & 0 & -s_{sh} & s_{sh} \end{pmatrix} \begin{pmatrix} \varphi_1 \\ \varphi_2 \\ \varphi_3 \\ \varphi_n \\ \varphi_{gen} \end{pmatrix} = \qquad (40)$$

where

φ_i Blade rotational angle with zero position for blade 1 0°, for blade 2 120°, f or blade 3 240°

φ_n, φ_{gen} Rotational angle for generator or nacelle respectively, zero position at 0°

θ Moment of inertia with respect to main shaft axis for blade i, nacelle and generator respectively

s_i Substitutional bending stiffness of blade i for in-plane direction

s_{sh} Main shaft torsional stiffness

T_i Rotor torque component caused by in-plane forces on blade i

T_{gen} Generator torque

The blades are represented by discrete single masses located at a given distance from the main shaft axis. This equation of motion can be decoupled by means of modal analysis (see Section 6.1) which yields independent equations, one for each mode.

Both generator speed and position are measured in common wind turbines with a high accuracy. These signals could be used to provide a correction input to the state estimator. Besides, the generator torque could be provided as an input signal. If strain measurements are available for a main shaft cross section (see Section 4.5), they can as well be used for the state-space estimation. However, apportioning the total aerodynamic torque on the three blades is difficult. Either a known proportion between the blades has to be assumed or additional information is necessary, which could be provided e.g. from blade root strain measurements, see Section 6.3.2.

6.6 Main Shaft Bending Loads and Main Bearing Radial Loads

The total main shaft bending is the superposition of lateral bending and vertical bending. There are two causes: Rotor gravitational forces and a rotor yaw and/or tilt moment. These two components are treated independently. Generally, by superposing the respectively arising stresses, the total load situation can be evaluated.

The main shaft bending load is strongly related to the main bearing's radial loads. It makes thus sense to estimate them within the same algorithm.

The main shaft bending load case is considered not to contain a relevant load component from structural motion. The estimation process is thus carried out using “static” physical models.

Figure 18 qualitatively shows the impact of rotor weight on the main shaft bending loads, where

$$F_{grav} \cdot d_{rot} = F_{2,grav} \cdot d_{bear} = -M_{b,shaft,grav,max} \tag{41}$$

and

$$F_{1,grav} = F_{grav} \frac{(d_{rot} + d_{bear})}{d_{bear}} \tag{42}$$

The resulting bending occurs in vertical direction only, however, due to the main shaft rotation, this static force leads to a periodically fluctuating, fatigue type load at constant amplitude, the frequency varying with rotor speed. The same is true for the inner bearing rings, which rotate with the shaft: They experience a fluctuating radial force with amplitude $F_{1,grav}$ and $F_{2,grav}$ respectively. In contrast, $F_{1,grav}$ and $F_{2,grav}$ present a constant load for the outer bearing rings.
Thanks to the known rotor weight (changes e.g. due to icing are neglected), the loads at any point of the shaft can be calculated continuously using the current rotor position and the mentioned dimensions.

Yet, the only way to mitigate this type of load by means of turbine control is to reduce rotor speed, and thus the number of load cycles. This issue is subject to general turbine design rather than short-term controlling.

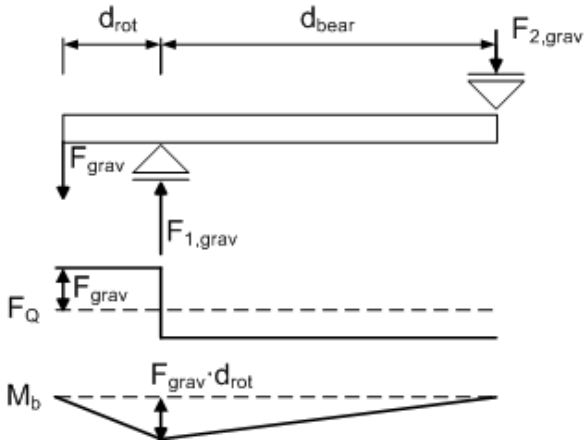

Figure 18: *Main Shaft Bending Loads Caused by Rotor Gravity*

The main shaft bending component caused by fluctuating yaw/tilt moments on the rotor can be estimated in a similar way if the current rotor yaw/tilt moments are known. For the case of the main shaft and the bearings, it makes sense to not treat the yaw and tilt moment independently but to combine them to a total rotor moment $M_{b,yt}$. Using the estimated or measured blade root bending moments and blade root shear forces (see Section 6.3.2), the total rotor moment can be retrieved by vectorial summation as in Equation (36).
Figure 19 illustrates the qualitative distribution of main shaft internal loads, which result from the total moment on the rotor for the static case. The force $F_{2,yt}$ and the total rotor moment are related by:

$$F_{2,yt} = \frac{M_{b,yt}}{d_{bear}} \tag{43}$$

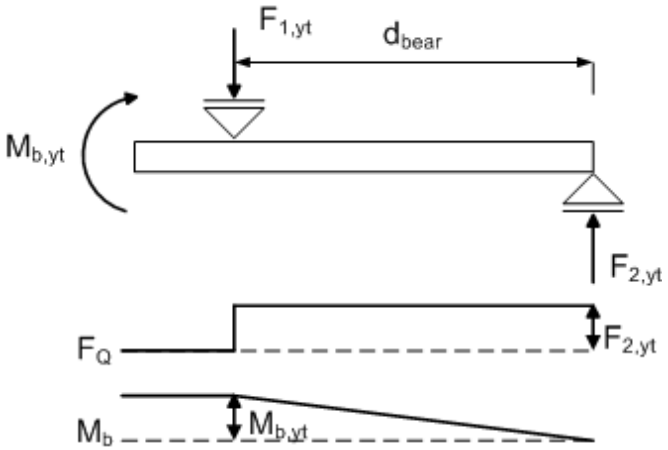

Figure 19: *Main Shaft Bending Loads Caused by a Rotor Yaw and Tilt Moment*

Since the total rotor moment typically fluctuates with respect to the main shaft, the resulting main shaft internal loads have a dynamic character. The same is true for the bearing inner rings. In turn, for a constant total rotor moment, the bearing outer rings experience constant loads.
They can be mitigated using a control algorithm to minimize the rotor total moment by means of cyclic or individual pitch control. Besides, permanent yaw misalignment can be reduced if the turbine control is continuously supplied with information on the rotor moment.

For the field of fault prediction, the total main shaft bending load is interesting to be monitored. In favour of this, a continuous Rainflow counting process can be performed for selected main shaft cross sections. For this, the loads resulting from both rotor gravity and rotor yaw/tilt moment have to be calculated continuously, considering the the current rotor position.

7. Conclusion and Future Work

An overview was given both over the mechanical loads on the most important turbine components and available sensor signals in wind turbines.
After an introduction to the field of load estimation, estimation methodologies were suggested for several turbine components, taking into account currently available sensor signals and those possibly available in future turbines. For several load cases, components were treated as “static” systems, i.e. structural motion was not considered for the internal load calculations. This approach simplifies load estimation and is suggested for the main shaft bending loads and bearing loads

The methodologies suggested for load cases with a significant share caused by component oscillations involve state-space estimators. The according load cases include blade and tower bending and drive train torsion. The estimators for the tower and drive train promise good estimation results. However, for blade bending, certain assumptions have to be made whose impacts on the estimation error are not known. Additional sensor signals over the blade might be necessary to reach a good estimation performance. Since tower bending, blade bending and drive train torsion are coupled, an overall state-space estimator will be considered in the future work, incorporating one comprehensive model for tower, blades and drive train and all relevant available sensor signals. Wind speed could be included as a disturbance model.

Generally, the accuracy of the mentioned estimation methodologies strongly depends on the accuracy of the models they are based on. Since wind turbines are nonlinear systems, linearisations have to be carried out for various operating points. Further, the system parameters depend on the site; e.g. the ambient temperature may differ or wind conditions may follow different patterns. Damage or wear causes time-variant system parameters; this has to be considered for a final estimator design e.g. by attaching importance to robustness.

8. References

[1] Baur, M., Modellierung und Regelung nichtlinearer dynamischer Mehrgrößensysteme auf der Basis von fuzzy-verknüpften lokalen linearen Modellen, Dissertation an der Technischen Universität Chemnitz, 2003

[2] Bensch, L., Enzinger, M., Jusseit, J., Kräftemessen am Himmel, dSpace News 3/2007

[3] Beitz, W., Grote, K.-H., Dubbel Taschenbuch für den Maschinenbau, Springer-Verlag, 1997

[4] Bossanyi, E.A., Garrad Hassan and Partners Ltd, Developments in Closed Loop Controller Design for Wind Turbines, American Institute of Aeronautics & Astronautics, 2000

[5] Burton, T., Sharpe, D., Jenkins, N., Bossanyi, E., Wind Energy Handbook, John Wiley & Sons, 2001

[6] Gasch, R., Knothe, K., Strukturdynamik Band 2, Springer-Verlag, 1989

[7] Immerkaer, N.P., Mortensen, I., LM Glasfiber A/S, Blade monitoring System, 2004

[8] Kim, D., Marciniak, M., A Methodology to Predict the Empennage In-Flight Loads of a General Aviation Aircraft Using Backpropagation Neural Networks, Office of Aviation Research, 2001

[9] Kowalczyk, K., Svaricek. F., Bohn, C., Disturbance-Observer-Based Active Control of Transmission-Induced Vibrations

[10] Krüger T., Regelungsverfahren für Windkraftanlagen zur Reduktion der mechanischen Belastung, Dissertation an der Universität Gesamthochschule Kassel, 1998

[11] Petko, M., Uhl, T., Smart Sensor for Operational Load Measurement, Transactions of the Institute of Measurement and Control 26, 2 (2004)

[12] Rademakers, L.W.M.M., Verbruggen, T.W., van der Werff, P.A., Korterink, H., Richon, D., Rey, P., Lancon, F., Fiber Optic Blade Monitoring

[13] Shkarayev, S., Krashantisa, R., Tessler, A., An Inverse Interpolation Method Utilizing In-Flight Strain Measurements for Determining Loads and Structural Response of Aerospace Vehicles

[14] Stol, K.A., Disturbance Tracking and blade Load Control of Wind Turbines in Variable-Speed Operation, AIAA/ASME Wind Symposium, Reno, 2003

[15] van Aken, J. M., Estimating Blade Section Airloads from Blade Leading-Edge Pressure Measurement, Proceedings of the American Helicopter Society 59th Annual Forum, Phoenix, 2003

[16] van der Hooft, E.L., van Engelen, T.G., Feed forward control of estimated wind speed, ECN-C-03-137, 2003

[17] Wright, A.D., Modern Control Design for Flexible Wind Turbines, Technical Report, National Renewable Energy Laboratory, Golden, 2004

[18] Zerbst, S., Entwicklung eines Schadensfrüherkennungssystems für Tragstrukturen von Windenergieanlagen, 2. Nationales PhD-Seminar der EAW, Hannover, 2007

The information on sensors contained in Section 3 and 4 are based on the following company websites:

http://www.baumerhuebner.com
http://www.meas-spec.com
http://www.mikrosensor.de
http://www.sensata.com
http://www.sensoren.de
http://www.mmf.de
http://www.insensys.com
http://www.pcb.com
http://www.smartfibres.com
http://www.thiesclima.com